TREET: TRansfer Entropy Estimation via Transformer

Omer Luxembourg, *Student Member, IEEE*, Dor Tsur, *Student Member, IEEE*,
Haim Permuter, *Senior Member, IEEE*

Abstract—**Transfer entropy (TE) is a measurement in information theory that reveals the directional flow of information between processes, providing valuable insights for a wide range of real-world applications. This work proposes Transfer Entropy Estimation via Transformers (TREET), a novel transformer-based approach for estimating the TE for stationary processes. The proposed approach employs Donsker-Vardhan (DV) representation to TE and leverages the attention mechanism for the task of neural estimation. We propose a detailed theoretical and empirical study of the TREET, comparing it to existing methods. To increase its applicability, we design an estimated TE optimization scheme that is motivated by the functional representation lemma. Afterwards, we take advantage of the joint optimization scheme to optimize the capacity of communication channels with memory, which is a canonical optimization problem in information theory, and show the memory capabilities of our estimator. Finally, we apply TREET to real-world feature analysis. Our work, applied with state-of-the-art deep learning methods, opens a new door for communication problems which are yet to be solved.**

Index Terms—**Deep Learning, Information Theory, Transfer Entropy, Transformers, Neural Estimation, Communication Channels**

I. INTRODUCTION

TRANSFER entropy (TE), introduced by Schreiber [1], stands as a pivotal information-theoretic measurement that captures the coupling dynamics within temporally evolving systems [2]. Derived from the principles of mutual information (MI), TE is distinctive for its inherent asymmetry, strategically employed in diverse applications for causal analysis [3]. TE serves as a robust measure of the directed, asymmetric information flow between two stochastic processes. Specifically, TE quantifies the reduction in uncertainty about prospective values, incorporating the past values of one process to predict the future values of another [4].

Transformers [5] are a neural network (NN) architecture that in recent years became prevalent in many fields of research, including time series forecasting [6]–[8]. With the attention mechanism, transformers are avoiding traditional recurrent flow of states, such in recurrent NNs (RNNs), with a bounded length of input sequence, yet manage to achieve great results [9].

The versatility of TE is evident in various domains. In neuroscience, it has proven to be effective in deciphering functional connectivity among neurons and between neurons to various physical tasks [10]–[12]. Moreover, analysis between

All authors are with the Department of Electrical and Computer Engineering of Ben-Gurion University of the Negev.

visual sensors and movement actuators in embodied cognitive systems can be one via TE [13]. TE proves indispensable as it empowers social networks to delve into the intricate dynamics of social influence and helps to encompass the spread of misinformation and scrutinize statistical causality in various text-related events, including the spread of misinformation [14]. [15] utilizes a variant of TE in conjunction with an RNN to predict the direction of the US stock market, incorporating TE as input feature. Lately [16] suggested a greedy algorithm for feature selection while leveraging the connection between each feature and the target with TE.

A. Estimation and Optimization of Transfer Entropy

Estimating information theoretic measures such as TE is challenging, due to lack of samples and unknown underlying distribution of the data, that may lead to larger errors in estimation [4]. Among the estimation methods, Kernel Density Estimation (KDE) [17], k-nearest neighbors (KNN) [18], [19], and the Kraskov-Stögbauer-Grassberger (KSG) technique are noteworthy, despite their struggle with the bias-variance trade-off. Notably, Granger causality [20] also serves as a foundational method for TE estimation, particularly in Gaussian joint processes where it is equivalent to TE, highlighting its effectiveness in quantifying information flow between sequences [21], [22].

Recent advancements have embraced neural estimation methods for information theory measures, leveraging the Donsker-Varadhan (DV) variational formula for Kullback-Leibler (KL) divergence to accurately estimate metrics like MI, directed information (DI) rate, and TE [23]–[26]. These methods, including MI neural estimation (MINE), DI neural estimation (DINE), and the intrinsic TE neural estimator (ITENE) for MI, DI rate and variant of TE respectively, utilize NNs to solve optimization problems, facilitating the estimation process even in complex scenarios, such as estimating the channel capacity of continuous channels in the presence of memory. However, challenges arise with larger context windows, necessitating adjustments for accurate estimation in broader historical contexts.

NNs have revolutionized fields such as computer vision and natural language processing, with transformers now leading time series analysis, overtaking RNNs due to their superior performance [6]–[8], [27]. Despite the widespread use of MINE for information measure estimation, it subjects to certain limitations that undergone comprehensive scrutiny [28]–[30]. To address these issues, our novel approach, inspired by

DINE, utilizes the capabilities of transformers. This method specifically tailors TE estimation to the sequential dynamics of data, offering a significant improvement over conventional techniques that overlook temporal relationships.

B. Contributions

In this work, we introduce TREET, a novel approach for estimating TE using transformers. Our method is grounded in the DV representation, leveraging attention-based NNs adapted to meet the structural constraints of DV optimization. Theoretically, we establish the consistency of TREET and develop an auxiliary neural distribution generator (NDG) module to facilitate TE optimization, utilizing transformers.

Empirically, we showcase the versatility of TREET across various applications. We present our findings on channel capacity estimation, illustrating the efficacy of the TREET and NDG in a joint optimization and estimation process, supported by theoretical validations. Additionally, we highlight the memory capabilities of TREET through a long memory channel example. A key empirical contribution is our feature analysis of the Apnea dataset, illustrating the potential of TREET for comprehensive real-world data analysis, paving the way for broader applications in future research.

C. Organizations

The paper is structured as follows, Section II provides background on information theory and NNs. Section III presents the TREET, it's theoretical guarantees and practical implementations, while the optimization of TREET is described in Section IV. Experimental results for channel capacity estimation, memory analysis and features analysis on physiological data are shown in Section V. Section VI concludes the paper and discuss future research potentials.

II. BACKGROUND

In this section, we elaborate on the preliminaries necessary to present our method. We familiarize the reader with our notation and provide the formal definition of TE, then relate it to DI. Subsequently, we introduce the concept of transformer NN, define them, and discuss the theorem of universal approximation. Lastly, we present the use of NN as estimators for information theory measurements.

A. Notation

Calligraphic letters, such as $\mathcal{X}$, denote subsets of the d-dimensional Euclidean space, $\mathbb{R}^d$. Expectations are represented by $\mathbb{E}$, with all random variables defined in the probability space $(\Omega, \mathcal{F}, \mathbb{P})$. The collection of Borel probability measures on $\mathcal{X}$ is indicated as $\mathcal{P}(\mathcal{X})$, and $\mathcal{P}_{\mathsf{ac}}(\mathcal{X})$ specifically refers to those measures that are absolutely continuous with respect to Lebesgue measure, with their densities denoted by lowercase p. Random variables and vectors are uppercase, e.g., X, and stochastic processes are in blackboard bold, e.g., $\mathbb{X} := (X_t)_{t\in\mathbb{Z}}$ for discrete time t.

The sequence of l samples from time t in process $\mathbb{X}$ is $X_t^{t+l} := [X_t, \ldots, X_{t+l}]^\top$, and for stationary processes,

$X^l := [X_1, \ldots, X_l]^\top$. For a measure $\mathcal{Q} \in \mathcal{P}_{\mathsf{ac}}(\mathcal{X})$ with PDF q, cross entropy between P and Q is $\mathsf{h}_{\mathsf{CE}}(P,Q) := -\mathbb{E}_P[\log q]$. Differential entropy of $X \sim P$ is $\mathsf{h}(X) := \mathsf{h}_{\mathsf{CE}}(P,P)$. If $Q \ll P$, the KL divergence $\mathsf{D}_{\mathsf{KL}}(P\|Q) := \mathbb{E}_P[\log \frac{\mathrm{d}P}{\mathrm{d}Q}]$. MI between $(X,Y) \sim P_{XY}$ is $\mathsf{I}(X;Y) := \mathsf{D}_{\mathsf{KL}}(P_{XY}\|P_X \otimes P_Y)$. Conditional KL divergence for $P_{Y|X}, Q_{Y|X}$ given $X \sim P_X$ is $\mathsf{D}_{\mathsf{KL}}(P_{Y|X}\|Q_{Y|X}|P_X)$, and conditional MI for $(X,Y,Z) \sim P_{XYZ}$ is $\mathsf{I}(X;Y|Z) := \mathsf{D}_{\mathsf{KL}}(P_{XY|Z}\|P_{X|Z} \otimes P_{Y|Z}|P_Z)$.

B. Transfer Entropy

TE quantifies causal influence from the past of one sequence on the present of another, formally given by

Definition 1 (Transfer Entropy) *For jointly distributed processes $\mathbb{X}$ and $\mathbb{Y}$ and $k, l < \infty$, the TE, with parameters (k,l), is given by*

$$\mathsf{TE}_{X\to Y}(t;k,l) := \mathsf{I}\left(X_{t-l}^t; Y_t|Y_{t-k}^{t-1}\right). \tag{1}$$

When the considered processes are jointly stationary, we can omit the temporal index t in (1) and write TE as

$$\mathsf{TE}_{X\to Y}(k,l) := \mathsf{I}\left(X^l; Y_l|Y_{l-k}^{l-1}\right). \tag{2}$$

Note that our definition of TE includes X_t, whereas other definitions [1], [21], [26], [31] define TE as $\mathsf{I}(X^{l-1}; Y_l|Y_{l-k}^{l-1})$. The main difference of this change is that our definition reduces to MI when the processes are jointly independent and identically distributed (i.i.d.), i.e., $\mathsf{TE}_{X\to Y}(0,0) = I(X;Y)$. When $k = l$, we use the abbreviated notation $\mathsf{TE}_{X\to Y}(l)$.

C. Relation to Directed Information

DI [32], [33] is given by

$$\mathsf{I}(X^n \to Y^n) := \sum_{i=1}^n \mathsf{I}\left(X^i; Y_i|Y^{i-1}\right)$$
$$= \sum_{i=1}^n \mathsf{TE}_{X\to Y}(i). \tag{3}$$

When (X^n, Y^n) are n-fold projections of some stochastic processes $\mathbb{X}$ and $\mathbb{Y}$ and from (2) we can observe that DI is the sum of TE. We can define the DI *rate*, which is given by

$$\mathsf{I}(\mathbb{X} \to \mathbb{Y}) := \lim_{n\to\infty} \frac{1}{n}\mathsf{I}(X^n \to Y^n)$$
$$\overset{(a)}{=} \lim_{n\to\infty} \mathsf{I}(X^n; Y_n|Y^{n-1}), \tag{4}$$

and (a) holds due to stationarity [25]. The DI rate can be therefore observed as a limit case of TE, where the limit of TE exists since $\mathsf{TE}_{X\to Y}(l) = \mathsf{h}(Y_l|Y^{l-1}) - \mathsf{h}(Y_l|X^l, Y^{l-1})$ and each conditional entropy is non-negative, decreasing for increasing l (conditioning reduces entropy). Moreover, under appropriate Markov assumptions, $Y_l - Y^{l-1} - Y_{-\infty}^{-1}, Y_l - (X^l, Y^{l-1}) - (X_{-\infty}^{-1}, Y_{-\infty}^{-1})$, we can form an equality between TE and DI (refer to Appendix VII-A for further details).

D. Attention Mechanism and Transformers

NNs serve as a universal function approximators [34], excelling in capturing complex relationships within the data. NNs

capabilities can be enhanced by the attention[1] mechanism [27], which selects various combinations of inputs according to their significance to the predictions. The attention can address time series datasets, while weighting over each time input. Attention comprises *queries*, which represent the current temporal focus, *keys*, which match against the queries to determine relevance, and *values*, that contain the NN inputs to be weighted and act as a memory function in time-series. Attention is formally given by

Definition 2 (Attention) *Let* $Q = XW_Q, K = XW_K$ *and* $V = XW_V$ $(W_Q, W_K, W_V \in \mathbb{R}^{x \times d})$ *be the queries, keys and values, which are linear projections of the input* $X = (x_1, x_2, \ldots, x_n)$, $\forall i : x_i \in \mathbb{R}^x$. *Then the attention is as follows,*

$$\mathsf{Attn}(X) = \mathsf{softmax}\left(QK^\top\right)V,$$

where $\mathsf{softmax}(Z)_j = \exp[Z_j]/\sum_{m=1}^{n} \exp[Z_m]$ *where* $Z \in \mathbb{R}^n$, *is performed for each column of the dot-product between queries and keys separately. The weights are calculated from the softmax operation and the output is weighted from the values* V.

Transformers utilize positional encoding (PE), which is a maps each input to the attention according to its ordinal index, and is usually applied before the attention for time series applications to deformation of the sequence structure. In addition, a generalization of the transformer uses multi-head attention,

$$\mathsf{MultiHead\text{-}Attn}(X) = [H_1, \ldots, H_h]W_0, \tag{5}$$

where

$$H_i = \mathsf{softmax}\left(Q^{(i)}K^{(i)^\top}\right)V^{(i)}, \quad i = 1, \ldots, n, \tag{6}$$

where $W_0 \in \mathbb{R}^{dh \times d}$ is learnable parameter, and $Q^{(i)}, K^{(i)}, V^{(i)}$ are the ith learnable projections of queries keys and values [27]. A transformer block is a sequence-to-sequence function, which maps input sequence of to an output sequence. Each transformer block consists of attention layer and time-wise feed-forward layer.

Formally, a transformer is given as follows.

Definition 3 (Transformer function class) *Let* $d_i, d_o, l, v \in \mathbb{N}$. *The class of transformers with* v *neurons, denoted* $\mathcal{G}_{\mathsf{tf}}^{(d_i, d_o, l, v)} : \mathbb{R}^{d_i \times l} \to \mathbb{R}^{d_o \times l}$, *is the set of discrete-time with the following structure:*

$$X_{\mathsf{pe}} = W_1 \cdot X + E, \tag{7a}$$

$$\mathsf{Attn}(X_{\mathsf{pe}}) = X_{\mathsf{pe}} + \sum_{i=1}^{h} W_O^i W_V^i X_{\mathsf{pe}}$$
$$\cdot \mathsf{softmax}\left[(W_K^i X_{\mathsf{pe}})^\top (W_Q^i X_{\mathsf{pe}})\right], \tag{7b}$$

$$Y = \mathsf{FF}(X_{\mathsf{pe}}) = \mathsf{Attn}(X_{\mathsf{pe}}) + W_3 \cdot \sigma_{\mathsf{R}}$$
$$\left(W_2 \cdot \mathsf{Attn}(X_{\mathsf{pe}}) + b_1 \mathbf{1}_l^\top\right) + b_2 \mathbf{1}_l^\top, \tag{7c}$$

where $X \in \mathbb{R}^{d_i \times l}$ *is the input sequence of* l *samples,* $Y \in \mathbb{R}^{d_o \times l}$ *is the transformer output,* $W_1 \in \mathbb{R}^{d_e \times d_i}, W_O^i \in \mathbb{R}^{d_e \times d_m}, W_Q^i, W_K^i, W_V^i \in \mathbb{R}^{d_m \times d_e}, W_2 \in \mathbb{R}^{d_r \times d_e}, W_3 \in$

$\mathbb{R}^{d_e \times d_r}, b_1 \in \mathbb{R}^{d_r}, b_2 \in \mathbb{R}^{d_e}$ *are the weights and biases of the network,* $E \in \mathbb{R}^{d_e \times l}$ *is the PE of the input. The number of heads* h *and the head size* d_m *are the parameters of the multi-head attention while* d_r *is the hidden dimension of the feed-forward (FF) layer. Assuming that the input is an additive product with it's positional encoding product, before the transformer blocks. The class of transformers with dimensions* (d_i, d_o, l) *is thus given by*

$$\mathcal{G}_{\mathsf{tf}}^{(d_i, d_o, l)} := \bigcup_{v \in \mathbb{N}} \mathcal{G}_{\mathsf{tf}}^{(d_i, d_o, l, v)}. \tag{8}$$

Transformers are a universal approximation class of sqeuence to sequence mappings:

Theorem 1 (Universal approx. for transformers) *Let* $\epsilon > 0$, $l \in \mathbb{N}$. $\mathcal{U} \subset \mathbb{R}^{T \times d_i}, \mathcal{Z} \subset \mathbb{R}^{l \times d_o}$ *be open sets, and* $f : \mathcal{U} \to \mathcal{Z}$ *be a continuous vector-valued function. Then, there exist* $v \in \mathbb{N}$ *and a* v-*neuron transformer* $g \in \mathcal{G}_{\mathsf{tf}}^{(d_i, d_o, l, v)}$ *(as in Definition 3, such that for any sequence of inputs* $\{u^l\} \in \mathcal{U}$ *and sequence of outputs* $\{z^l\} \in \mathcal{Z}$, *we have*

$$\left\| f(u^l) - g(u^l) \right\|_1 \le \epsilon, \tag{9}$$

This paper utilizes the class of *causal transformers*, $\mathcal{G}_{\mathsf{ctf}}$, which is built upon $\mathcal{G}_{\mathsf{tf}}$. To this end, we use the notion of causal functions

Definition 4 (Causal Function) *Let* $\mathcal{F} : \mathbb{R}^{d_u \times L} \to \mathbb{R}^{d_z \times L}$ *be a function for* $d_u, d_z, L \in \mathbb{N}$. *For a series of inputs* $U = \{u_t\}_{t=1}^{L}$ *and function outputs* $Z = \{z_t\}_{t=1}^{L}$, *the function* $\mathcal{F}$ *is defined as a causal function iff, for any* $t_0, t \in \{1, \ldots, L\}, t \le t_0$, *the output* z_{t_0} *depends only on the inputs* u_t.

In order to achieve a causal mapping function, we apply *causal mask* on the attention scores, to result with a mapping that overlooks dependence on future elements as in Definition 4 (note that only the attention perform time mixing, thus leaving the rest of the transformers intact is valid). The causal mask, denoted as $M \in \mathbb{R}^{l \times l}$, multiplied element-wise with the dot-product of keys and queries, before the softmax operation, and is given by

$$M_{[i,j]} = \begin{cases} 1 & \text{if } j \le i \\ -\infty & \text{otherwise} \end{cases} \tag{10}$$

where $-\infty$ nullifies the corresponding entries after the softmax operation. Hence, (7b) is written as,

$$\mathsf{Attn}(X_{\mathsf{pe}}) = X_{\mathsf{pe}} + \sum_{i=1}^{h} W_O^i W_V^i X_{\mathsf{pe}}$$
$$\cdot \mathsf{softmax}\left[(W_K^i X_{\mathsf{pe}})^\top (W_Q^i X_{\mathsf{pe}}) \odot M\right]. \tag{11}$$

Although changing the dot-product operation of the attention, the model remains consistent with the universality framework, which is grounded in the architecture's capacity for pair-wise operations rather than being constrained by the specifics of the attention mechanism [5]. Thus, zeroing out elements in the input sequence aligns with the transformers function class.

E. Neural Estimation

Neural estimation is a methodology that utilizes NN optimization for the optimization of various functionals. First introduced by the MINE, neural estimators often utilize the DV representation [23, Theorem 3.2].

Theorem 2 (DV representation) *For any, $P, Q \in \mathcal{P}(\mathcal{X})$, we have*

$$D_{\mathsf{KL}}(P\|Q) = \sup_{f:\mathcal{X}\to\mathbb{R}} \mathbb{E}_P[f] - \log\left(\mathbb{E}_Q[e^f]\right), \quad (12)$$

where the supremum is taken over all measurable functions f with finite expectations.

The MINE is then obtained by approximating the DV optimization function class with the class of NNs, and estimating expectations with samples means. The MINE was generalized to additional information theoretic quantities, such as conditional MI [35], total correlation [36], and TE with its variations [26]. Furthermore, a generalization of the MINE to DI was proposed in [25]. Drawing inspiration from the MI and DI neural estimators, we develop a provably consistent estimator of TE that utilizes the power of the attention mechanism.

III. ESTIMATION OF TRANSFER ENTROPY

In this paper we harness to computational power of transformers architecture and modify the attention mechanism to result with TREET, a new estimator of TE for high dimensional continuous data. We begin by deriving the estimator, then account for its theoretical guarantees. Finally, we provide implementation details, outlining the modifications of attention to neural estimation.

A. Estimator Derivation

The TREET provides an estimate of the TE (1) from a set of samples $D_{n,l} = (X^{n+l}, Y^{n+l}) \sim P_{X^{n+l}, Y^{n+l}}$. We assume that $l \ll n$ and this omit the dependence on l in the dataset notation. The TREET decomposes TE into two KL terms, each of which taken between the the data distribution and a corresponding reference distribution $\widetilde{P}_Y$, such that $\widetilde{P}_Y$ can be sampled freely. To derive TREET, first we represent TE as subtraction of KL divergences w.r.t. and absolutely continuous $\widetilde{P}_Y$. We propose the following.

Lemma 1 (TE as KL Divergences) *TE decomposes as*

$$\mathsf{TE}_{X\to Y}(l) = \mathsf{D}_{Y_l|Y^{l-1}X^l\|\widetilde{Y}_l} - \mathsf{D}_{Y_l|Y^{l-1}\|\widetilde{Y}_l}, \quad (13)$$

where

$$\mathsf{D}_{Y_l|Y^{l-1}\|\widetilde{Y}_l} := \mathsf{D}_{\mathsf{KL}}\left(P_{Y_l|Y^{l-1}}\|\widetilde{P}_{Y_l}\Big|P_{Y^{l-1}}\right), \quad (14a)$$

$$\mathsf{D}_{Y_l|Y^{l-1}X^l\|\widetilde{Y}_l} := \\ \mathsf{D}_{\mathsf{KL}}\left(P_{Y_l|Y^{l-1}X^l}\|\widetilde{P}_{Y_l}\Big|P_{Y^{l-1}X^l}\right), \quad (14b)$$

and the conditional KL divergence is $\mathsf{D}_{\mathsf{KL}}(P_{X|Z}\|P_{Y|Z}|P_Z) := \mathbb{E}_Z[\mathsf{D}_{\mathsf{KL}}(P_{X|Z}\|P_{Y|Z})]$.

Lemma 1 is proved in Section VII-C, and follows basic information theoretic properties of TE and KL divergences.

Utilizing the DV variational representation (12) and performing the optimization over a set of causal transformer architectures $\mathcal{G}_{\mathsf{ctf}}^Y := \mathcal{G}_{\mathsf{ctf}}^{(d_y,1,l,v_y)}, \mathcal{G}_{\mathsf{ctf}}^{XY} := \mathcal{G}_{\mathsf{ctf}}^{(d_x+d_y,1,l,v_{xy})}$ for given $l, d_y, d_x, v_y, v_{xy} \in \mathbb{N}$, and let $g_y \in \mathcal{G}_{\mathsf{ctf}}^Y, g_{xy} \in \mathcal{G}_{\mathsf{ctf}}^{XY}$. Each KL divergence can be approximated with transformers by

$$\mathsf{D}_{Y_l|Y^{l-1}\|\widetilde{Y}_l} = \sup_{g_y\in\mathcal{G}_{\mathsf{ctf}}^Y} \mathbb{E}\left[g_y\left(Y^l\right)\right] \\ - \log\left(\mathbb{E}\left[e^{g_y\left(\widetilde{Y}_l,Y^{l-1}\right)}\right]\right), \quad (15a)$$

$$\mathsf{D}_{Y_l|Y^{l-1}X^l\|\widetilde{Y}_l} = \sup_{g_{xy}\in\mathcal{G}_{\mathsf{ctf}}^{XY}} \mathbb{E}\left[g_{xy}\left(Y^l, X^l\right)\right] \\ - \log\left(\mathbb{E}\left[e^{g_{xy}\left(\widetilde{Y}_l,Y^{l-1},X^l\right)}\right]\right). \quad (15b)$$

Finally, replacing expectations with sample means in (15), we result with the TREET, given by

$$\widehat{\mathsf{TE}}_{X\to Y}(D_n; l)$$

$$:= \sup_{g_{xy}\in\mathcal{G}_{\mathsf{ctf}}^{XY}} \sup_{g_y\in\mathcal{G}_{\mathsf{ctf}}^Y} \widehat{\mathsf{TE}}_{X\to Y}(D_n, g_y, g_{xy}; l) \quad (16a)$$

$$= \sup_{g_{xy}\in\mathcal{G}_{\mathsf{ctf}}^{XY}} \widehat{\mathsf{D}}_{Y_l|Y^{l-1}X^l\|\widetilde{Y}_l}(D_n, g_{xy})$$

$$- \sup_{g_y\in\mathcal{G}_{\mathsf{ctf}}^Y} \widehat{\mathsf{D}}_{Y_l|Y^{l-1}\|\widetilde{Y}_l}(D_n, g_y), \quad (16b)$$

where

$$\widehat{\mathsf{D}}_{Y_l|Y^{l-1}\|\widetilde{Y}_l}(D_n, g_y) := \frac{1}{n}\sum_{i=1}^n g_y\left(Y_i^{i+l}\right) \\ - \log\left(\frac{1}{n}\sum_{i=1}^n e^{g_y\left(\widetilde{Y}_{i+l},Y_i^{i+l-1}\right)}\right), \quad (17a)$$

$$\widehat{\mathsf{D}}_{Y_l|Y^{l-1}X^l\|\widetilde{Y}_l}(D_n, g_{xy}) := \frac{1}{n}\sum_{i=1}^n g_{xy}\left(Y_i^{i+l}, X_i^{i+l}\right) \\ - \log\left(\frac{1}{n}\sum_{i=1}^n e^{g_{xy}\left(\widetilde{Y}_{i+l},Y_i^{i+l-1},X_i^{i+l}\right)}\right). \quad (17b)$$

where $\widetilde{Y}$ is i.i.d. under absolutely continuous reference measurement under the alphabet $\mathcal{Y}$, and $\sup_{g_{xy}\in\mathcal{G}_{\mathsf{ctf}}^{XY}} \widehat{\mathsf{D}}_{Y_l|Y^{l-1}X^l\|\widetilde{Y}_l}(D_n, g_{xy}) = \mathsf{D}_{Y_l|Y^{l-1}X^l\|\widetilde{Y}_l}$, $\sup_{g_y\in\mathcal{G}_{\mathsf{ctf}}^Y} \widehat{\mathsf{D}}_{Y_l|Y^{l-1}\|\widetilde{Y}_l}(D_n, g_y) = \mathsf{D}_{Y_l|Y^{l-1}\|\widetilde{Y}_l}$. The TREET (16b) is consequently given as the subtraction of the solutions of two optimization problems (17), each optimizing its own NN. The optimization is then performed via gradient ascent with the corresponding model g_y, g_{xy} and the dataset D_n. Note that Definition 15 states that each KL divergence we estimate with DV representation, achieved by function of $(Y^l, \widetilde{Y}_l)$ and $(Y^l, X^l, \widetilde{Y}_l)$, thus we use a causal transformer to opt g_y, g_{xy} in order to ignore relative future values of the process. In the following section, we prove that the TREET implemented with causal transformers is a consistent estimator of TE.

B. Theoretical Guarantees

To further understand the capabilities of TREET, we explore its theoretical guarantees. Assuming joint stationarity of $(\mathbb{X}, \mathbb{Y})$
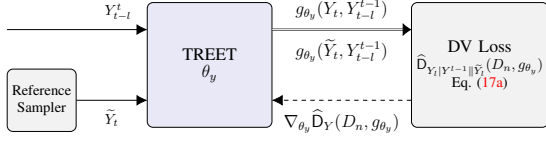
Fig. 1: The estimator architecture for the calculation of $\widehat{\mathsf{D}}_{Y_l|Y^{l-1}\|\widetilde{Y}_l}(D_n, g_{\theta_y})$.

and using the causal transformers function class, we introduce the consistency of the proposed TREET.

Theorem 3 (TREET consistency) *Let $\mathbb{X}$ and $\mathbb{Y}$ be jointly stationary, ergodic stochastic processes. TREET is strongly consistent estimator of $\mathsf{TE}_{X\to Y}(l)$ for $l \in \mathbb{N}$, i.e. $\mathbb{P} - a.s.$ for every $\epsilon > 0$ there exists and $N \in \mathbb{N}$ such that for every $n > N$ we have*

$$\left| \widehat{\mathsf{TE}}_{X\to Y}(D_n; l) - \mathsf{TE}_{X\to Y}(l) \right| \leq \epsilon \tag{18}$$

where l is the memory parameter of the TE.

The proof following the steps of representation step - represents TE as a subtraction of two DV potentials, estimation step - proves that the DV potentials is achievable by empirical mean of a given set of samples, and approximation step - shows that the estimator built upon causal transformers converges to TE with the corresponding memory parameter. The proof is given in the Appendix VII-B.

C. Algorithm and Implementation

This section describes the TREET implementation. We present an overview scheme for estimation of TE and describe the algorithm. Afterwards we show the architecture of the TREET and going deeper to its implementation. Formally, the transformer function class is parametric models whose finitely many parameters are a subset of a parameter space $\Theta \subset \mathbb{R}^d, d \in \mathbb{N}$. For a fixed $v < \infty$ neurons, denote the functions from the above classes as $g \in \mathcal{G}_v$, or their corresponding parameterized form $g_\theta, \theta \in \Theta$. We therefore denote the corresponding networks with $g_{\theta_y}, g_{\theta_{xy}}$, where θ_y and θ_{xy} are the network parameters, respectively. We now describe the algorithm design and transformer modifications.

1) Overview and Algorithm: The TREET algorithm follows an iterative joint optimization of $\widehat{\mathsf{D}}_{Y_l|Y^{l-1}X^l\|\widetilde{Y}_l}$ and $\widehat{\mathsf{D}}_{Y_l|Y^{l-1}X^l\|\widetilde{Y}_l}$ through iterative mini-batch gradient optimization. The algorithm inputs are l, D_n, which are the TE parameter and the dataset, respectively. Every iteration begins with feeding mini-batch sized $m < n$ with sequences length l in each model, followed by the calculation of both DV potentials (17), that construct $\mathsf{TE}_{X\to Y}(l)$ (16a). The calculated objective is then used for gradient-based optimization of the NN parameters. The iterative process continues until a stopping criteria is met, typically defined as the convergence of $\mathsf{TE}_{X\to Y}(l)$ within a specified tolerance parameter $\epsilon > 0$. For evaluation, we produce the estimated TE again for many samples as possible, and taking the averaged results. The full pipeline for estimating $\widehat{\mathsf{D}}_{Y_l|Y^{l-1}X^l\|\widetilde{Y}_l}(D_n, g_{\theta_y})$ is presented in
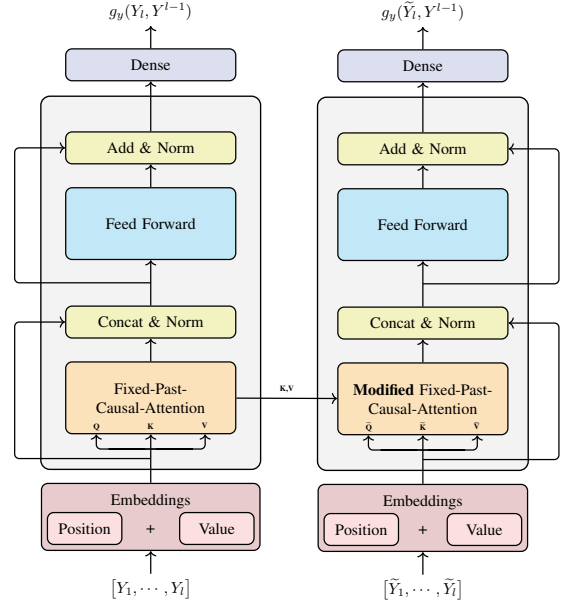

Fig. 2: The TREET architecture for g_y, with memory parameter l. It illustrated using a single sequence as an example. However, it is capable of parallel processing for sequences lengthed $L > l$, and in such cases, the number of outputs for the function will be $L - l + 1$. Both transformer share the same weights. The FPCA and the modified FPCA are as elaborated in Section III-C2.

Algorithm 1 TREET

Input: Joint process samples D_n; Observation length $l \in \mathbb{N}$.
Output: $\widehat{\mathsf{TE}}_{X\to Y}(D_n; l)$ - TE estimation.

1: NNs initialization $g_{\theta_y}, g_{\theta_{xy}}$ with corresponding parameters θ_y, θ_{xy}.
2: **Step 1 – Optimization:**
3: **repeat**
4:   Draw a batch B_m: $m < n$ sub-sequences, length $L > l$ from D_n, with reference samples $P_{\widetilde{Y}}$ for each.
5:   Compute both potentials $\widehat{\mathsf{D}}_{Y_l|Y^{l-1}X^l\|\widetilde{Y}_l}(B_m, g_{\theta_{xy}})$, $\widehat{\mathsf{D}}_{Y_l|Y^{l-1}\|\widetilde{Y}_l}(B_m, g_{\theta_y})$ via (17).
6:   Update parameters:
7:     $\theta_{xy} \leftarrow \theta_{xy} + \nabla_{\theta_{xy}} \widehat{\mathsf{D}}_{Y_l|Y^{l-1}X^l\|\widetilde{Y}_l}(B_m, g_{\theta_{xy}})$
8:     $\theta_y \leftarrow \theta_y + \nabla_{\theta_y} \widehat{\mathsf{D}}_{Y_l|Y^{l-1}\|\widetilde{Y}_l}(B_m, g_{\theta_y})$
9: **until** convergence criteria.
10: **Step 2 – Evaluation:** Evaluate for a sub-sequence (17) and (16a) to obtain $\widehat{\mathsf{TE}}_{X\to Y}(D_n; l)$.

Figure 1, and the complete list of steps is given in Algorithm 1.

The DV representation, (12), suggest that the function f is the same function for both terms that construct it, i.e. the weights are shared for both network propagation. Hence, our transformer in TREET, which constructed by (17), is the same for both terms, for both DV representation. Exemplifying with $\widehat{\mathsf{D}}_{Y_l|Y^{l-1}\|\widetilde{Y}_l}$, both $g_y(Y^l)$ and $g_y(\widetilde{Y}^l, Y^{l-1})$ use the same learning parameters, from positional encoding layers and attention to FF layers. The only difference we have between

$$QK^\top = \begin{bmatrix} q_{(t+l)} \cdot k_{(t)} & \cdots & q_{(t+l)} \cdot k_{(t+l)} & -\infty & \cdots & -\infty \\ -\infty & q_{(t+l+1)} \cdot k_{(t+1)} & \cdots & q_{(t+l+1)} \cdot k_{(t+l+1)} & -\infty & \vdots \\ \vdots & -\infty & \ddots & & \ddots & -\infty \\ -\infty & \cdots & -\infty & q_{(t+L)} \cdot k_{(t+L-l)} & \cdots & q_{(t+L)} \cdot k_{(t+L)} \end{bmatrix} \tag{19}$$

$$\widehat{QK^\top} = \begin{bmatrix} \widetilde{q}_{(t+l)} \cdot k_{(t)} & \cdots & \widetilde{q}_{(t+l)} \cdot \widetilde{k}_{(t+l)} & -\infty & \cdots & -\infty \\ -\infty & \widetilde{q}_{(t+l+1)} \cdot k_{(t+1)} & \cdots & \widetilde{q}_{(t+l+1)} \cdot \widetilde{k}_{(t+l+1)} & -\infty & \vdots \\ \vdots & -\infty & \ddots & & \ddots & -\infty \\ -\infty & \cdots & -\infty & \widetilde{q}_{(t+L)} \cdot k_{(t+L-l)} & \cdots & \widetilde{q}_{(t+L)} \cdot \widetilde{k}_{(t+L)} \end{bmatrix}. \tag{20}$$

the two terms, is in how we operate the attention mechanism, which essentially re-use keys and values generated for the first term, to generate the later one. This model for g_y is visualized in Figure 2. The following sections will elaborate about the proposed *fixed past causal attention* (FPCA) that constructs the TREET and its variation, *modified fixed past causal attention* which is required for the reference measurement sampling.

2) Fixed Past Causal Attention : In this section we describe the calculation of $g_y(Y^l)$ (17a). For $L > l$, the causal attention architecture is constructed by queries $Q \in \mathbb{R}^{L \times d_o}$, keys $K \in \mathbb{R}^{L \times d_o}$ and values $V \in \mathbb{R}^{L \times d_o}$, and given by

$$Q = [q_1, \ldots, q_L]^\top, \quad K = [k_1, \ldots, k_L]^\top,$$
$$V = [v_1, \ldots, v_L]^\top, \tag{21}$$

where $L \in \mathbb{N}$ is the temporal length of the model's input and $l \in \mathbb{N}$ is the memory parameter which determines $\mathsf{TE}_{X \to Y}(l)$. The ith step queries, keys and values in the are given by $q_i = W_Q x_i, k_i = W_K x_i, v_i = W_V x_i$, and $M \in \mathbb{R}^{L \times L}$, thus we denote

$$\text{Causal-Attention} := \text{softmax}(QK^\top \odot M)V. \tag{22}$$

To result in a valid causal attention mechanism and fixed length input size l, we propose the FPCA, where each query will be multiplied only by its relative time key and past $l-1$ keys. Thus the dot-product operation is between $[t+l, t+L]$ queries time steps and $[t, t+L]$ keys time steps. In addition, we change the causal mask (i.e. for the above case $M \in \mathbb{R}^{L-l \times L}$) to a Toeplitz-like band matrix mask $M' \in \mathbb{R}^{L-l \times L}$,

$$M'_{[i,j]} = \begin{cases} 1 & \text{if } j - i < l \text{ and } j \geq i \\ -\infty & \text{otherwise} \end{cases} \tag{23}$$

The resulting queries and keys dot-product with the given mask yields (19), and the FPCA is given by

$$\text{FPCA} := \text{softmax}(QK^\top \odot M')V \tag{24}$$

Note that we use only the last $L - l + 1$ results from the transformer outputs sequence, in order to keep the past information fix to length l. With the given FPCA, the required DV output $g_y(Y^l)$ can be calculated.

3) Reference Sampling with FPCA: This section describes the calculation of $g_y(\widetilde{Y}_l, Y^{l-1})$ (17a). As mentioned in Section III-A, the reference distribution, $\widetilde{Y}$, is independently drawn

from some absolute continuous PDF over the bounds of $\mathcal{Y}$[2]. Denote the scoring value after the softmax operation of causal attention for query q_i with key k_j as

$$\mathcal{R}_{(i,j)} := \frac{e^{q_i \cdot k_j}}{\sum_{m=1}^{i} e^{q_i \cdot k_m}}, \quad j \leq i. \tag{25}$$

Since we use FPCA with memory parameter l, the output at time t can be written as $\mathsf{FPCA}_t = \mathcal{R}_{(t,t-l)} v_{t-l} + \mathcal{R}_{(t,t-l+1)} v_{t-l+1} + \ldots + \mathcal{R}_{(t,t)} v_t$. In order to calculate $g_y(\widetilde{Y}_t, Y_{t-l}^{t-1})$, the output of the time mixing must contain the original distribution from past information up to time step $t-1$. This information is stored in the keys and values of the previous resulted FPCA_t, for $g_y(Y_{t-l}^t)$. Thus, the modified FPCA should be constructed by

$$\widetilde{\mathcal{R}}_{(i,j)} := \begin{cases} \frac{e^{\widetilde{q}_i \cdot k_j}}{e^{\widetilde{q}_i \cdot \widetilde{k}_i} + \sum_{m=1}^{i-1} e^{\widetilde{q}_i \cdot k_m}} & , i \neq j \\ \frac{e^{\widetilde{q}_i \cdot \widetilde{k}_i}}{e^{\widetilde{q}_i \cdot \widetilde{k}_i} + \sum_{m=1}^{i-1} e^{\widetilde{q}_i \cdot k_m}} & , i = j. \end{cases} \tag{26}$$

In this case, the modified FPCA can be written as Modified-$\mathsf{FPCA}_t = \widetilde{\mathcal{R}}_{(t,t-l)} v_{t-l} + \widetilde{\mathcal{R}}_{(t,t-l+1)} v_{t-l+1} + \ldots + \widetilde{\mathcal{R}}_{(t,t)} \widetilde{v}_t$, for time t. Summarizing, the second term (17a) generated by the modified FPCA, contains all keys and values of the relative past and query, key and value for the current present, which is a function of the reference distribution. The dot-product matrix between queries and keys can be written as (20), for $l \leq L$, and modified FPCA is written as Modified-FPCA $= \text{softmax}(\widehat{QK^\top} \odot M')V$.

The extension of FPCA and modified FPCA to multi-head version is immediate. In our implementation, the reference inputs, for the second term in (17a) are drawn from the uniform measure on the bounding box of the current batch of Y samples, while theoretically, our method allows to draw from any positive continuous distribution measure; for further details check Appendix VII-B. The implementation of $\widehat{\mathsf{D}}_{Y_l|Y^{l-1}X^l\|\widetilde{Y}_l}(D_n, g_{xy})$ (17b) is obtained by concatenating the X^l values with the corresponding Y^l or $\widetilde{Y}^l$ values for both the FPCA and the modified FPCA, respectively.

IV. OPTIMIZATION OF ESTIMATED TRANSFER ENTROPY

Many applications can leverage the optimization of TE, in a given data-driven setting. The optimization of which can

---

[2]If $\mathcal{Y}$ is not bounded, we set manually the maximal bounds regarding to the dataset properties.
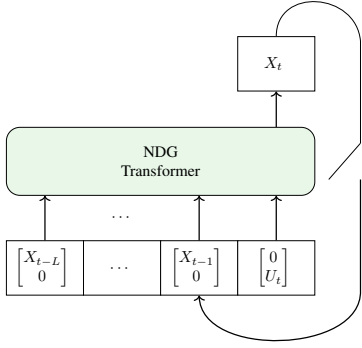
Fig. 3: The recursive process for the NDG with transformers. If feedback presents, the input includes the past channel output, concatenated with the corresponding value X_i at time i.
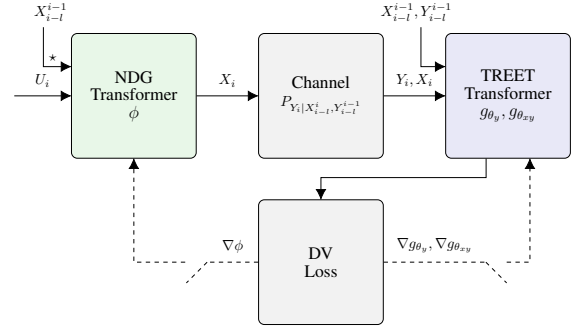

Fig. 4: Complete system for estimating and optimizing TREET with NDG while Altering between the models to train on. ($\star$) If feedback presents, past channel output realizations included.

be done via controlling the distribution of the process $\mathbb{X}$ and $\mathbb{Y}$, independently or jointly. An important example for such a setting would be communication channels, whose capacity can be characterized with a certain TE term.

Remark 1 (Channel capacity) *As presented in [25], consider channels with and without feedback links from the channel output back to the encoder. The feedforward capacity of a channel sequence $\left\{ P_{Y^n \| X^n} \right\}$, for $n \in \mathbb{N}$ is*

$$C_{\mathsf{FF}} = \lim_{n \to \infty} \sup_{P_{X^n}} \frac{1}{n} \mathsf{I}(X^n; Y^n), \qquad (27)$$

while the feedback capacity is

$$C_{\mathsf{FB}} = \lim_{n \to \infty} \sup_{P_{X^n \| Y^{n-1}}} \frac{1}{n} \mathsf{I}(X^n \to Y^n). \qquad (28)$$

The achievability of the capacities is further discussed in [37], [38]. [32] showed that for non-feedback scenario, the optimization problem over $P_{X^n \| Y^n}$ can be translated to P_{X^n}, which support the use of DI rate for both optimization problems. Under some conditions TE can estimate the capacity as well, as presented in Section II-C.

Focusing on channel capacity, we assume that we can control the input distribution sampling mechanism and propose an algorithm for the optimization of estimated TE with respect to the input generator. We refer to this model as the *Neural Distribution Generator* (NDG). The estimated TE optimization methodology is inspired by the proposed methods from [25]. However, the adaptation to transformer architectures considers a different implementation of the proposed scheme. As the TREET estimates TE from samples, the NDG is defined as a generative model of the input distribution samples, and is optimized with the goal of maximizing the downstream estimated TE.

Lemma 2 (Optimal TE) *Let $(\mathbb{X}, \mathbb{Y})$ be jointly stationary processes, and the TE with memory parameter $l \in \mathbb{N}$. Then, the maximal TE, $\mathsf{TE}^\star_{X \to Y}(l)$, by $\mathbb{X}$ is*

$$\mathsf{TE}^\star_{X \to Y}(l) := \sup_{P_{X^l}} \mathsf{I}(X^l; Y_l | Y^{l-1}). \qquad (29)$$

The proof of the lemma is given in Appendix VII-D. The

lemma suggests that NDG with input sequence length l is enough to achieve maximum TE with memory parameter l, for independently controlling the distribution of $\mathbb{X}$.

The NDG calculates a sequence of channel input X^l through the mapping

$$h_\phi : (U_i, Z_{i-l}^{i-1}) \to X_i^\phi, \qquad i = 1, \dots, n, \qquad (30)$$

where U_i is the random noise drawn from $P_U \in \mathcal{P}_{\mathsf{ac}}(\mathcal{U}), \mathcal{U} \subset \mathbb{R}^{d_x}$, which cause the stochasticity, Z_{i-l}^{i-1} are the past observation of the generated process created by the model, and the channel corresponding outputs if feedback exists, and h_ϕ is the parametric NDG mapping with parameters $\phi \in \Phi$. By the functional representation lemma [39] and the restated lemma in [25], we can achieve the distribution of X from an NN function. After l iterations, with Z_{i-l}^{i-1} storing the relevant information of previous iterations, the NDG generates the whole sequence. Transformers need access to the whole sequence at once, in contrast to RNNs where a single state can theoretically represent the past sequence.

Thus, the input sequence to the NDG with transformer is created via past outputs of the transformer itself (and corresponding channel outputs if feedback exists) as depicted in Figure 3, and the past observations are taken without gradients to prevent backpropagation through iterations. In our implementation, the input convention for each time step is a concatenated vector of $[X_i, U_i]^\top$ to maintain the input structure of samples and random noise for every projection in the network, while in relative history time steps, the noise is replaced with zero, and for the present time, the input X_i is replaced with a zero vector of the same dimension.

To estimate and optimize the TE at once, we jointly training the TREET and the NDG. As described in Algorithm 2 and Figure 4, in each iteration we only update one of those models by maximizing each DV potentials, $\widehat{\mathsf{D}}_{Y_l | Y^{l-1} \| \widetilde{Y}_l}, \widehat{\mathsf{D}}_{Y_l | Y^{l-1} X^l \| \widetilde{Y}_l}$, for TREET model and by maximizing $\widehat{\mathsf{TE}}_{X \to Y}$ for NDG model. The entire pipeline of one iteration will create a sequence length l from the NDG, by iterating it l times with some initiated zero values - which creates the dataset, $D_n^\phi = (X^{\phi,n}, Y^{\phi,n})$. Afterwards, feeding each sample sequence from the dataset to TREET for achieving the corresponding networks' outputs as mentioned back in Algorithm 1, which constructs the loss that will gen-

Algorithm 2 Continuous TREET optimization

Input: Continuous sequence-to-sequence system $\mathcal{S}$; Observation length $l \in \mathbb{N}$.
Output: $\widehat{\mathsf{TE}}^{\star}_{X \to Y}(U^n; l)$, optimized NDG.

1: NNs initialization g_{θ_y}, $g_{\theta_{xy}}$ and h_ϕ with corresponding parameters $\theta_y, \theta_{xy}, \phi$.
2: **repeat**
3:    Draw noise U^m, $m < n$.
4:    Compute batch B_m^ϕ sized m using NDG, $\mathcal{S}$
5:    **if** training TREET **then**
6:       Perform TREET optimization - Step 1 in Algorithm 1.
7:    **else** Train NDG
8:       Compute $\widehat{\mathsf{TE}}_{X \to Y}(B_m^\phi, g_{\theta_y}, g_{\theta_{xy}}, h_\phi; l)$ using (16a).
9:       Update NDG parameters:
10:      $\phi \leftarrow \phi + \nabla_\phi \widehat{\mathsf{TE}}_{X \to Y}(B_m^\phi, g_{\theta_y}, g_{\theta_{xy}}, h_\phi; l)$
11: **until** convergence criteria.
12: Draw U^m to produce l length sequence and evaluate $\widehat{\mathsf{TE}}_{X \to Y}(D_n^\phi; l)$.
13: **return** $\widehat{\mathsf{TE}}^{\star}_{X \to Y}(U^n; l)$, optimized NDG.

erate gradients backward according to each model. Next, we demonstrate the power of the proposed method for estimating the channel capacity.

V. EXPERIMENTAL RESULTS

In this section we demonstrate the utility and performance of the proposed algorithms to several tasks, encompasing both estimation and optimization of TE. Additionally, we perform a comparison with the RNN-based DI rate estimation scheme from [25] and discusses the results. While the experiments are about continuous spaces of distributions, discrete spaces can easily be applied to the algorithm of TREET, but not for the optimization part with NDG as presented. The TREET consists of transformer with a single fixed-past-causal-attention layer follows by a single FF layer, and the NDG also consists of transformer with a single causal-attention layer and a single FF layer. Further details on the implementation parameters are provided in Appendix VII-E. All simulations are implemented in PyTorch and the code implementation can be found at this repository: https://github.com/omerlux/TREET.

A. Empirical Capacity Estimation for Finite Memory Processes

As shown in Section II-C, under some conditions TE is equal to the DI rate and converges to it. DINE [25] proved that it can estimate a capacity of stationary channels by optimizing the DI rate estimator and the input distribution of the channel P_X, as Remark 1 mentions about channel capacities. Our experiments has shown that for memory-less channels and for memory channels with and without feedback, TREET can approximate the capacity with the joint optimization procedure of the input distribution (NDG) and TE estimation. Important to note that channel input constraints are essential for ensuring that the transmitted signals are well-suited to the channel's
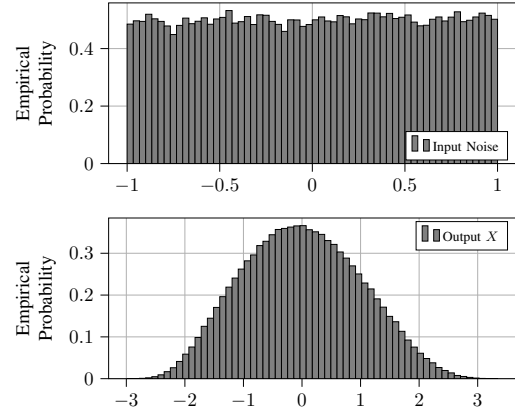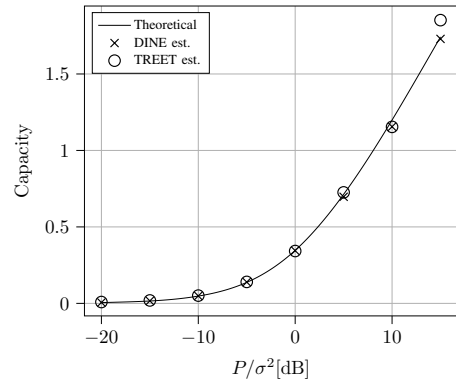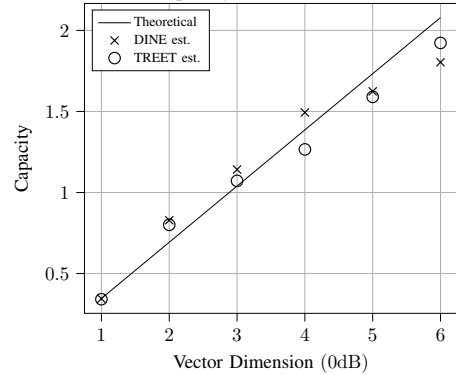

Fig. 5: NDG input noise and output X, 0 SNR case.

(a) Capacity as function of SNR.

(b) Capacity as function of vector dimension.

Fig. 6: Channel capacity estimation of AWGN channel. 6a presents the estimation of TREET and DINE in comparison to theoretical capacities for various SNR rates. P represents the power constraint and the noise parameter is σ^2. 6b shows the capacity estimation with variate vector process dimension for the 0 dB case. For the case of power constraint $P = 1$ theoretically the input P_X distributes $\mathcal{N}(0,1)$.

characteristics and limitations. In our experiment we applied the power constraint on the input signal of the channel, which is implemented via normalizing a batch of samples to a certain statistics according to the power constraint.
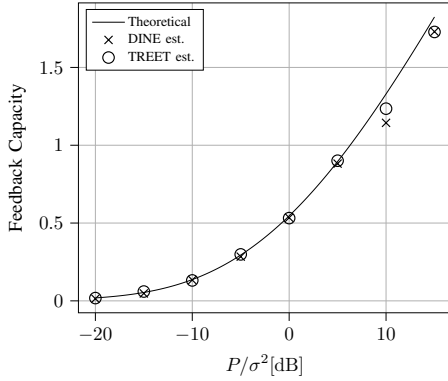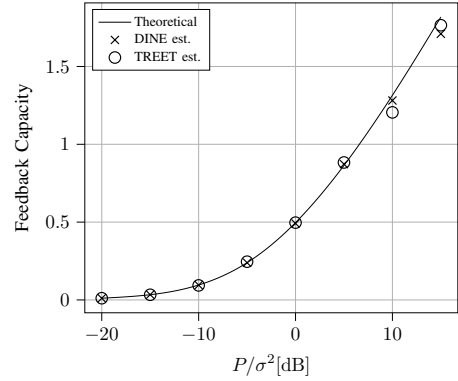
(a) Feedback Capacity.
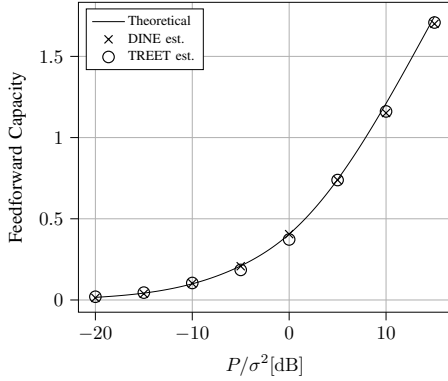
(b) Feedforward Capacity.

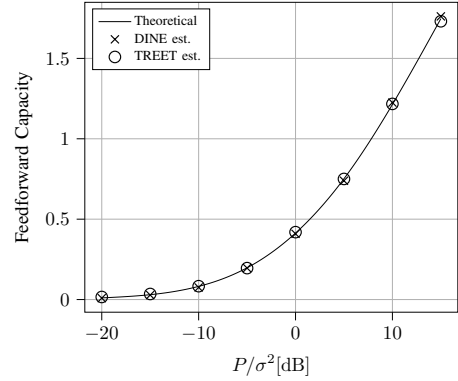Fig. 7: Channel capacity estimation of Gaussian MA(1) channel with variate SNR.

(a) Feedback Capacity.

(b) Feedforward Capacity.

Fig. 8: Channel capacity estimation of Gaussian AR(1) channel with variate SNR.

1) AWGN Channel: Consider additive white Gaussian noise (AWGN) channel with i.i.d. noise,

$$Z_i \sim \mathcal{N}(0, \sigma^2),$$
$$Y_i = X_i + Z_i, \qquad i \in \mathbb{Z},$$

X_i is the channel's input sequence, coupled with the average power constraint $\mathbb{E}[X_i^2] \leq P$. The capacity of this channel is simple for analytical calculation, and is given by the following formula $C = 0.5 \log \left(1 + P/\sigma^2\right)$. Since the process is memoryless, maximized both DI rate and TE (for any $l \geq 0$) coincide with the channel capacity. We estimated and optimized the TREET according to Algorithm 2 and compared the model performance with the DI rate estimation and optimization scheme from [25]. Results are presented in Figure 6. It can be seen that both are estimating the right capacities which are the MI, although their access to multiple past observations, and in addition, the dimension of the input vector and output vector of a channel changes the capacities, as expected. Note that larger dimensions cause error of in estimation and still is an open academic research [28]. To further analyse the learned distribution, we visualize the optimized NDG mapping in Figure 5. It can be seen that the optimized NDG maps the uniform ($U \sim [-1,1]$) inputs into Gassian samples. This observation meets our expectations, as the capacity achieving AWGN distribution is Gaussian [40].

2) Gaussian MA(1) Channel: Given a Moving Average (MA) Gaussian noise channel with order 1

$$Z_i = N_i + \alpha N_{i-1},$$
$$Y_i = X_i + Z_i, \qquad i \in \mathbb{Z},$$

where $N_i \sim \mathcal{N}(0, \sigma^2)$ are i.i.d. and X_i is the input to the channel with power constraint $\mathbb{E}[X_i^2] \leq P$. We apply Algorithm 2 to both feedforward and feedback settings, comparing with ground truth solutions and the DI-based scheme. The feedforward capacity can be calculated with the water-filling algorithm [34], while the feedback capacity can be calculated by the root of forth order polynomial equation [41]. As seen in Figure 7 our method successfully estimated the capacity for a wide range of SNR values.

3) Gaussian AR(1) Channel: The case of autoregressive (AR) Gaussian noise channel of order 1 is similar,

$$Z_i = N_i + \alpha Z_{i-1},$$
$$Y_i = X_i + Z_i, \qquad i \in \mathbb{Z},$$

where $N_i \sim \mathcal{N}(0, \sigma^2)$ are i.i.d. and X_i is the input to the channel with power constraint $\mathbb{E}[X_i^2] \leq P$. The capacity is also affected by the existence of feedback. Feedforward capacity can be solved with the water-filling algorithm [34] and [42] prove how to achieve the feedback capacity analytically. Figure 8 compares the results of DINE and TREET estimators.
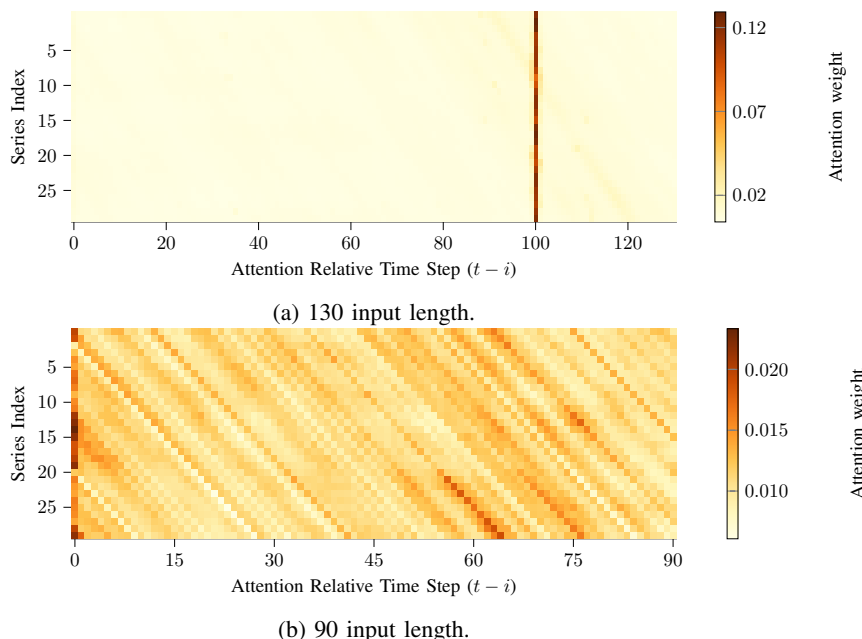
(a) 130 input length.

(b) 90 input length.

Fig. 9: Attention weights at training convergence of TREET optimized by NDG. Each row in the matrices represent a different input sequence and the columns are the weights of past values i from current prediction t (i.e. $i = 0$ represent the present prediction t). For the GMA(100) process, it can be observed that giving enough time-steps, TREET easily observes at the related time $i = 100$ where the information needed to be gathered from, while shorter length lead to instability of training.

B. Memory Capabilities Analysis

Previous experiments showed the capability of correctly estimating TE. Delving deeper into the memory effectiveness of TREET, we tested Gaussian MA channel, as presented before, but with time delay of 100 steps.

$$Z_i = N_i + \alpha N_{i-100},$$
$$Y_i = X_i + Z_i, \qquad i \in \mathbb{Z}.$$

It is notable that to achieve the correct capacity, the information from $t - 100$ steps must be an input to the TREET. We tested the estimation optimization algorithm with shorter input length and longer input length, than the demanded one. Figure 9a shows the analysis of the attention weights related to the $\widehat{D}_{Y_l|Y^{l-1}X^l\|\widetilde{Y}_l}$ model with $l = 130$ input steps for the estimation, at the late stages of training close to convergence, while Figure 9b considers the same for $l = 90$ input steps. It is evident from Figure 9 that TREET captures relevant information even from very long time series, while shorter length will lead larger error of information extraction which cause a worse estimation result, which is rational due to trimming of critical information.

Additionally, we compare TREET with DINE for different input lengths on the GMA(100) channel. Important to note that DINE can technically deal with long sequences even if given a shorter backpropagation through time (*bptt*) input length then the process memory is due to state propagation. However, as seen in Table I, the DINE struggles to estimate the right capacity under long memory, while TREET successfully estimates capacity with low error rate. Nonetheless, when the TREET memory is shorter than the channel memory, its performance significantly degrades.

| Model	Memory Length	Estimated Capacity [nits]	Absolute Error (%)
DINE	90	0.3435	15.3 (%)
TREET	90	0.2962	26.9 (%)
DINE	130	0.3333	17.8 (%)
TREET	130	**0.3851**	**5.0** (%)

TABLE I: GMA(100), with 0 SNR, capacity estimation with different lengths. Note that memory length in DINE is the *bptt* length for LSTM, while in TREET it is the sequence input length.

C. Transfer Entropy Estimation in Physiological Data

Motivated by the results in [4, Chapter 7.1], we tested the TREET on the Apnea dataset from Santa Fe Time Series Competition[3] [43], [44]. This is a multivariate data that has been recorded from a diseased patient of Apnea in a sleep laboratory, which is a condition characterized by brief, involuntary pauses in breathing, particularly during sleep. Each sample consists of three different variables from a specific time, with a sample rate of 2 Hz. The three features are heart rate, chest volume (which is the respiration force) and blood oxygen concentration. A sampled sequence of heart rate and breath rate (chest volume) is presented in Figure 10a.

Determining the interaction between different physiological features is crucial for diagnosing diseases by revealing causal connections within the human body, enabling targeted diagnostics and personalized treatments according to identified

[3]https://physionet.org/content/santa-fe/1.0.0/
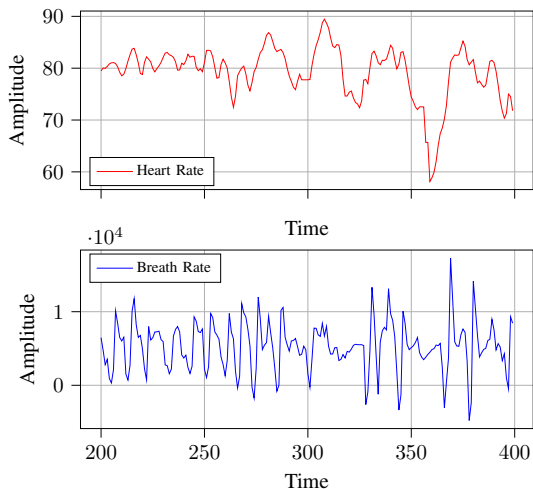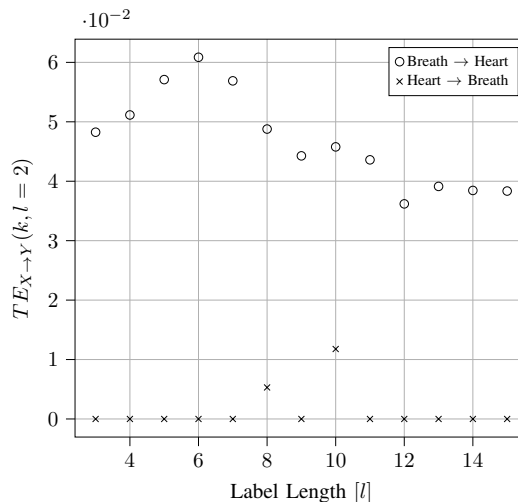
(a) Sampled sequence of Apnea dataset.

(b) TE estimation for variable length history of Y.

Fig. 10: Transfer Entropy estimation on physiological data. Apnea dataset consists of heart rate and breath rate and we seek to find the information flow for patient diagnosing. Patient with Apnea suffer from breathing cessation which leads to alterations in heart rate during sleep.

risk factors. Therefore, we applied the TREET to determine the magnitude and direction of information transfer in the given setting. We used both heart rate and breath features and compared the TE measurements, $\mathsf{TE}_{\mathsf{Breath}\to\mathsf{Heart}}(k, 2)$ and $\mathsf{TE}_{\mathsf{Heart}\to\mathsf{Breath}}(k, 2)$ for variable length k that is the Y process's history observations length. The results are presented in Figure 10b and are aligned with the results of [4] (for $k, l = 2$) and extend it further with tests on variate history length of Y process.

Notably, for every considered k, the TE from the breath process to the heart process is consistently higher, aligning with the diagnosis of Apnea disorder (abrupt cessation of breathing during sleep). In terms of information flow, our results indicate that the breathing process transfers more information regarding the behavior of the heart rate process, than the opposite direction, since the value of the estimated TE is consistently higher in comparison, while in information theory it essentially reflect that the X process has more to reveal about Y's current value than Y's past itself.

Furthermore, in the influence direction $\mathsf{TE}_{\mathsf{Breath}\to\mathsf{Heart}}$, we can infer that increasing the of visible heart rate history samples decreases the information transfer, since a longer history of heart rate provides more insight into future outcomes than the instantaneous breath value. However, $\mathsf{TE}_{\mathsf{Heart}\to\mathsf{Breath}}$ shows that for variate k values, the majority of TE results indicate that the heart process barely affect the breathing process in Apnea patients.

The conclusion of this experiment is very valuable and validates what is known to science - although it is known that when the heart rate increases the breath rate increases also, for Apnea patients, the sudden cessation of muscle movement during inhalation, i.e., the stopping of breathing, affects the heart rate, in contrast to what is observed in healthy individuals. This experiment supports the results of [4] and add a new insight about the information transfer decreasing

for increasing context of Y process (which reveals more information about Y, thus will lead to lower value of TE as mentioned before).

VI. CONCLUSIONS AND FUTURE WORK

This work presented a modified attention-based architecture to estimate TE, for a class of ergodic and stationary processes. We devise a DV-based neural TE estimator, proved its consistency and described the proposed novel modified attention mechanism for the task at hand. We then developed an optimizer of estimated TE, which was then leveraged for the estimation of channel capacity. We concluded by studying the TREET application in causal features analysis on the Apnea dataset and compared its performance with RNN-based mechanisms.

With the increasing popularity of sequential data to most contemporary fields of machine learning, we plan to leverage the TREET for information theoretic analysis and design of architectures, through the lenses of causal information transfer. Examples of such applications include enhancing predictive models, refining feature selection processes, reconstructing complex networks, improving anomaly detection capabilities, and optimizing decision-making in dynamic environments. Furthermore, building upon the work in [45], we plan to extend the TREET optimization scheme to sequential data compression tasks.

VII. APPENDIX

A. Lemma TE Equals to DI

Lemma 3 *Define markov property $Z_n - Z_{n-1} - Z^{n-2}$ as $P_{Z_n|Z^{n-1}} = P_{Z_n|Z_{n-1}}$. Let $\mathbb{X}$ and $\mathbb{Y}$ be two jointly stationary processes such that the following markov property holds,*

$$Y_l - Y^{l-1} - Y_{-\infty}^0,$$
$$Y_l - (X^l, Y^{l-1}) - (X_{-\infty}^0, Y_{-\infty}^0),$$

for $l \in \mathbb{N}$. *Then,*

$$\mathsf{TE}_{X \to Y}(m) = \mathsf{TE}_{X \to Y}(l) \qquad (31)$$

for $m \geq l$ *and*

$$\mathsf{TE}_{X \to Y}(m) = \mathsf{I}\left(\mathbb{X} \to \mathbb{Y}\right). \qquad (32)$$

proof: Let $\mathbb{X}$, $\mathbb{Y}$ be two jointly stationary processes that pose the markov property with $l \in \mathbb{N}$ and $m \geq l$, then

$$
\begin{aligned}
&\mathsf{TE}_{X \to Y}(l) \\
&= \mathsf{I}\left(X^l; Y_l | Y^{l-1}\right) \\
&\overset{(a)}{=} \mathsf{I}\left(X_{l-m}^l; Y_l | Y_{l-m}^{l-1}\right) \\
&\overset{(b)}{=} \mathsf{I}\left(X^m; Y_m | Y^{m-1}\right) \\
&= \mathsf{TE}_{X \to Y}(m),
\end{aligned} \qquad (33)
$$

where (a) is true from the markovity, and (b) transition is index shift, and is valid due to stationarity of the process. Observing the DI rate,

$$
\begin{aligned}
&\mathsf{I}((\mathbb{X} \to \mathbb{Y}) \\
&\overset{(a)}{=} \lim_{n \to \infty} \frac{1}{n} \sum_{i=1}^{n} \mathsf{I}\left(X^i; Y_i | Y^{i-1}\right) \\
&= \lim_{n \to \infty} \frac{1}{n} \sum_{i=1}^{n} \left[\mathsf{h}\left(Y_i | Y^{i-1}\right) - \mathsf{h}\left(Y_i | X^i, Y^{i-1}\right)\right] \\
&\overset{(b)}{=} \lim_{n \to \infty} \mathsf{h}\left(Y_n | Y^{n-1}\right) - \mathsf{h}\left(Y_n | X^n, Y^{n-1}\right) \\
&= \lim_{n \to \infty} \mathsf{I}\left(X^n; Y_n | Y^{n-1}\right) \\
&\overset{(c)}{=} \lim_{n \to \infty} \mathsf{TE}_{X \to Y}(n) \\
&\overset{(d)}{=} \mathsf{TE}_{X \to Y}(m),
\end{aligned} \qquad (34)
$$

where the limit in (a) exists whenever the joint process is stationary, transition (b) is valid because the limit exists for each series of conditional entropies, and since conditioning reduces entropy, the limit for each normalized sum of series is $\lim_{n \to \infty} \mathsf{h}\left(Y_n | Y^{n-1}\right), \lim_{n \to \infty} \mathsf{h}\left(Y_n | X^n, Y^{n-1}\right)$, respectively [40, Theorem 4.2.1]. Since the limit exists for the conditional MI, transition (c) is valid by definition of TE, and the TE with limit of parameter m exists, and (d) is from (33) for $n \geq m$. Concluding the proof. $\square$

B. Proof of theorem 3

The proof following the steps of representation step - represents TE as a subtraction of two DV potentials, estimation step - proves that the DV potentials is achievable by empirical mean of a given set of samples, and approximation step - shows that the estimator converges to TE with the corresponding memory parameter l. Thus concluding that our estimator is a consistent estimator for the TE.

Let $\{X_i, Y_i\}_{i \in \mathbb{Z}}$ be the two values of a process $\mathbb{X}, \mathbb{Y}$ respectively, and $\mathbb{P}$ be the stationary ergodic measure over $\sigma(\mathbb{X}, \mathbb{Y})$. Define $P_{X^n, Y^n} := \mathbb{P}|_{\sigma(X^n, Y^n)}$ as the n-coordinate projection of $\mathbb{P}$, where $\sigma(X^n, Y^n)$ is the σ-algebra generated by (X^n, Y^n). Let $D_n = (X^n, Y^n) \sim P_{X^n, Y^n}$. Let $\widetilde{Y} \sim Q_Y$ be an absolutely continuous PDF, independent of

$\{(X_i, Y_i)\}_{i \in \mathbb{Z}}$ and its distribution noted as $\widetilde{P}_Y$. The proof is divided to three steps - variational representation, estimation from samples and functional approximation.

1) Representation of TE: In order to write TE as a difference between two KL divergences, recall Lemma 1 - let,

$$\mathsf{D}_{Y_l | Y^{l-1} \| \widetilde{Y}_l} := \mathsf{D}_{\mathsf{KL}}\left(P_{Y_l | Y^{l-1}} \| \widetilde{P}_{Y_l} \Big| P_{Y^{l-1}}\right), \qquad (35a)$$

$$\mathsf{D}_{Y_l | Y^{l-1} X^l \| \widetilde{Y}_l} := \mathsf{D}_{\mathsf{KL}}\left(P_{Y_l | Y^{l-1} X^l} \| \widetilde{P}_{Y_l} \Big| P_{Y^{l-1} X^l}\right). \qquad (35b)$$

Then

$$\mathsf{TE}_{X \to Y}(l) = \mathsf{D}_{Y_l | Y^{l-1} X^l \| \widetilde{Y}_l} - \mathsf{D}_{Y_l | Y^{l-1} \| \widetilde{Y}_l}. \qquad (36)$$

This lemma is proved in Section VII-C. Estimating the KL divergence is applicable with the DV representation 2

$$
\begin{aligned}
\mathsf{D}_{Y_l | Y^{l-1} \| \widetilde{Y}_l} = \sup_{f_y : \Omega_{\mathcal{Y}} \to \mathbb{R}} & \mathbb{E}\left[f_y\left(Y^l\right)\right] \\
& - \log \mathbb{E}\left[e^{f_y\left(Y^{l-1}, \widetilde{Y}_l\right)}\right],
\end{aligned} \qquad (37a)
$$

where $\Omega_{\mathcal{Y}} = \mathcal{Y}^l$. For the other term, the DV representation is,

$$
\begin{aligned}
\mathsf{D}_{Y_l | Y^{l-1} X^l \| \widetilde{Y}_l} = \sup_{f_{xy} : \Omega_{\mathcal{X} \times \mathcal{Y}} \to \mathbb{R}} & \mathbb{E}\left[f_{xy}\left(X^l, Y^l\right)\right] \\
& - \log \mathbb{E}\left[e^{f_{xy}\left(X^l, Y^{l-1}, \widetilde{Y}_l\right)}\right],
\end{aligned} \qquad (37b)
$$

where $\Omega_{\mathcal{X} \times \mathcal{Y}} = \mathcal{X}^l \times \mathcal{Y}^l$. The next section refers to (37a) but the claims are the same for (37b).

2) Estimation: By the DV representation, the supremum in (37a) achieved for

$$
\begin{aligned}
f_{y,l}^{\star} &:= \log\left(\frac{dP_{Y^l}}{d(P_{Y^{l-1}} \otimes \widetilde{P}_{Y_l})}\right) \\
&= \log p_{Y_l | Y^{l-1}} - \log \widetilde{p}_{Y_l},
\end{aligned} \qquad (38)
$$

where the last equality holds due to $P_{Y^l} \ll P_{Y^{l-1}} \otimes \widetilde{P}_{Y_l}$, both measures have Lebesgue densities. While it is not mandatory to select the reference measurement as uniform, choosing a uniform reference measurement can result in a constant that can be neutralized to obtain the likelihood function of $Y_l | Y^{l-1}$. This approach allows for simplification and facilitates the estimation process. Empirical means can estimate the expectations in (37a), while applying the generalized Birkhoff theorem [46], stated next:

Theorem 4 (The generalized Birkhoff theorem) *Let T be a metrically transitive 1 - 1 measure preserving transformation of the probability space $(\Omega, \mathcal{F}, \mathbb{P})$ onto itself. Let $g_0(\omega), g_1(\omega), \ldots$ be a sequence of measurable functions on Ω converging a.s. to the function $g(\omega)$ such that $\mathbb{E}[\sup_i |g_i|] \leq \infty$. Then,*

$$\frac{1}{n} \sum_{i=1}^{n} g_i(T^i \omega) \overset{n \to \infty}{\longrightarrow} \mathbb{E}[g], \quad \mathbb{P} - a.s. \qquad (39)$$

By applying Theorem 4 and for any $\epsilon > 0$ and sufficiently large n, we have

$$\left| \mathbb{E}\left[f_{y,l}^{\star}\left(Y^l\right)\right] - \frac{1}{n} \sum_{i=0}^{n-1} f_{y,l}^{\star}\left(Y_i^{i+l}\right) \right| < \frac{\epsilon}{8}, \qquad (40a)$$

$$\left| \log\left(\mathbb{E}\left[e^{f^{\star}_{y,l}(Y^{l-1},\widetilde{Y}_l)}\right]\right) \right.$$
$$\left. - \log\left(\frac{1}{n}\sum_{i=0}^{n-1}e^{f^{\star}_{y,l}(Y_i^{i+l-1},\widetilde{Y}_{i+l})}\right)\right| < \frac{\epsilon}{8}, \qquad (40b)$$

where $\{f^{\star}_{y,l}\}$ is the function of l time steps, that achieves the supremum of $\mathsf{D}_{\mathsf{KL}}\left(P_{Y_l|Y^{l-1}}\|\widetilde{P}_{Y_l}\Big|P_{Y^{l-1}}\right)$. Convergence achieved from the generalized Brikhoff theorem, where the series of functions is the fixed function $f^{\star}_{y,l}$,

$$\mathbb{E}_n\left[f^{\star}_{y,l}\left(Y^l\right)\right] := \frac{1}{n}\sum_{i=0}^{n-1}f^{\star}_{y,l}\left(Y_i^{i+l}\right), \qquad (41a)$$

$$\mathbb{E}_n\left[e^{f^{\star}_{y,l}(Y^{l-1},\widetilde{Y}_l)}\right] := \frac{1}{n}\sum_{i=0}^{n-1}e^{f^{\star}_{y,l}(Y_i^{i+l-1},\widetilde{Y}_{i+l})}. \qquad (41b)$$

3) Approximation: Last step is to approximate the functional space with the space of transformers. Recall that set of causal transformer architectures $\mathcal{G}^{Y}_{\mathsf{ctf}} := \mathcal{G}^{(d_y,1,l,v_y)}_{\mathsf{ctf}}, \mathcal{G}^{XY}_{\mathsf{ctf}} := \mathcal{G}^{(d_x+d_y,1,l,v_{xy})}_{\mathsf{ctf}}$ for given $l, d_y, d_x, v_y, v_{xy} \in \mathbb{N}$. Define

$$\widehat{\mathsf{D}}_{Y_l|Y^{l-1}\|\widetilde{Y}_l}(D_n) := \sup_{g_y\in\mathcal{G}^{Y}_{\mathsf{tf}}} \frac{1}{n}\sum_{i=0}^{n-1}g_y\left(Y_i^{i+l}\right)$$
$$- \log\left(\frac{1}{n}\sum_{i=0}^{n-1}e^{g_y(Y_i^{i+l-1},\widetilde{Y}_{i+l})}\right), \qquad (42)$$

where the DV functions are transformers $g_y \in \mathcal{G}^{Y}_{\mathsf{ctf}}, g_{xy} \in \mathcal{G}^{XY}_{\mathsf{ctf}}$. We want to prove that for a given $\epsilon > 0$

$$\left|\widehat{\mathsf{D}}_{Y_l|Y^{l-1}\|\widetilde{Y}_l}(D_n) - \mathsf{D}_{Y_l|Y^{l-1}\|\widetilde{Y}_l}\right| \leq \frac{\epsilon}{2}. \qquad (43)$$

From Theorem 2, we obtain

$$\mathbb{E}\left[f^{\star}_{y,l}\left(Y^l\right)\right] = \mathsf{D}_{Y_l|Y^{l-1}\|\widetilde{Y}_l}, \qquad (44a)$$

$$\mathbb{E}\left[f^{\star}_{y,l}\left(Y^{l-1},\widetilde{Y}_l\right)\right] = 1. \qquad (44b)$$

Thus, we bound the term following $\left|\widehat{\mathsf{D}}_{Y_l|Y^{l-1}\|\widetilde{Y}_l}(D_n) - \mathbb{E}\left[f^{\star}_{y,l}\left(Y_i^{i+l}\right)\right]\right|$. By the identity $\log(x) \leq x - 1, \forall x \in \mathbb{R}_{\geq 0}$ we gain

$$\left|\widehat{\mathsf{D}}_{Y_l|Y^{l-1}\|\widetilde{Y}_l}(D_n) - \mathbb{E}\left[f^{\star}_{y,l}\left(Y^l\right)\right]\right|$$
$$= \left| -\mathbb{E}\left[f^{\star}_{y,l}\left(Y^l\right)\right] + \sup_{g_y\in\mathcal{G}^{Y}_{\mathsf{tf}}} \left\{\frac{1}{n}\sum_{i=0}^{n-1}g_y\left(Y_i^{i+l}\right)\right.\right.$$
$$\left.\left. -log\left(\frac{1}{n}\sum_{i=0}^{n-1}e^{g_y(Y_i^{i+l-1},\widetilde{Y}_{i+l})}\right)\right\}\right|$$
$$\leq \left| 1 - \mathbb{E}\left[f^{\star}_{y,l}\left(Y^l\right)\right] + \sup_{g_y\in\mathcal{G}^{Y}_{\mathsf{tf}}} \left\{\frac{1}{n}\sum_{i=0}^{n-1}g_y\left(Y_i^{i+l}\right)\right.\right.$$
$$\left.\left. - \left(\frac{1}{n}\sum_{i=0}^{n-1}e^{g_y(Y_i^{i+l-1},\widetilde{Y}_{i+l})}\right)\right\}\right|$$
$$\leq \left| +\mathbb{E}\left[f^{\star}_{y,l}\left(Y^{l-1},\widetilde{Y}_l\right)\right] - \mathbb{E}\left[f^{\star}_{y,l}\left(Y^l\right)\right]\right.$$
$$\left. + \sup_{g_y\in\mathcal{G}^{Y}_{\mathsf{tf}}} \left\{\frac{1}{n}\sum_{i=0}^{n-1}g_y\left(Y_i^{i+l}\right)\right.\right.$$

$$\left.\left. - \left(\frac{1}{n}\sum_{i=0}^{n-1}e^{g_y(Y_i^{i+l-1},\widetilde{Y}_{i+l})}\right)\right\}\right|. \qquad (45)$$

Due to (40), there exists $N \in \mathbb{N}$ such that $\forall n > \mathbb{N}$

$$\left|\mathbb{E}\left[f^{\star}_{y,l}\left(Y^l\right)\right] - \mathbb{E}_n\left[f^{\star}_{y,l}\left(Y^l\right)\right]\right| < \frac{\epsilon}{8}, \qquad (46a)$$

$$\left|\left(\mathbb{E}\left[e^{f^{\star}_{y,l}(Y^{l-1},\widetilde{Y}_l)}\right]\right) - \mathbb{E}_n\left[e^{f^{\star}_{y,l}(Y^{l-1},\widetilde{Y}_l)}\right]\right| < \frac{\epsilon}{8}. \qquad (46b)$$

Plugging (46) to (45) gives

$$\left|\widehat{\mathsf{D}}_{Y_l|Y^{l-1}\|\widetilde{Y}_l}(D_n) - \mathsf{D}_{Y_l|Y^{l-1}\|\widetilde{Y}_l}\right|$$
$$\leq \frac{\epsilon}{4} + \left| -\mathbb{E}_n\left[e^{f^{\star}_{y,l}(Y^{l-1},\widetilde{Y}_l)}\right] - \mathbb{E}_n\left[f^{\star}_{y,l}\left(Y^l\right)\right]\right.$$
$$+ \sup_{g_y\in\mathcal{G}^{Y}_{\mathsf{tf}}} \left\{\frac{1}{n}\sum_{i=0}^{n-1}g_y\left(Y_i^{i+l}\right)\right.$$
$$\left.\left. - \left(\frac{1}{n}\sum_{i=0}^{n-1}e^{g_y(Y_i^{i+l-1},\widetilde{Y}_{i+l})}\right)\right\}\right|. \qquad (47)$$

Since the empirical mean of $f^{\star}_{y,l}$ is converging to the expected mean, it is uniformly bounded by some $M \in \mathbb{R}_{\geq 0}$. Since the exponent function is Lipschitz continuous with Lipschitz constant $\exp[M]$ on the interval $(-\infty, M]$, we obtain

$$\frac{1}{n}\sum_{i=1}^{n}e^{f^{\star}_{y,l}(\widetilde{Y}_{i+l},Y_i^{i+l-1})} - e^{g_y(\widetilde{Y}_l,Y_i^{i+l-1})}$$
$$\leq e^{M}\frac{1}{n}\sum_{i=1}^{n}\left|f^{\star}_{y,l}\left(\widetilde{Y}_{i+l},Y_i^{i+l-1}\right)\right.$$
$$\left. - g_y\left(\widetilde{Y}_{i+l},Y_i^{i+l-1}\right)\right|. \qquad (48)$$

Definition 4 is a sub-functions class of the continuous sequence to sequence functions class, and applies to the causal transformer. Thus, concludes that the causal transformer $g \in \mathcal{G}^{(d_i,d_o,l,v)}_{\mathsf{ctf}}$ also applies for the universal approximation theorem, for continuous vector-values functions. Moreover, for our case the output sequence is a scalar value, $\mathcal{U} \subset \mathbb{R}^{l\times d_i}, \mathcal{Z} \subset \mathbb{R}^{1\times d_o}$. For given ϵ, M, l and n, denote $g^{\star}_y \in \mathcal{G}^{(d_y,1,l,v)}_{\mathsf{ctf}}$ the Causal transformer, such that the approximation error is uniformly bounded $\exp[-M] \times \epsilon/4$ for the final time prediction out from the model. Finally, combining Theorem 1 we have

$$\left|\widehat{\mathsf{D}}_{Y_l|Y^{l-1}\|\widetilde{Y}_l}(D_n) - \mathsf{D}_{Y_l|Y^{l-1}\|\widetilde{Y}_l}\right|$$
$$\leq \left(1 + e^{M}\right)\frac{1}{n}\sum_{i=1}^{n}\left|f^{\star}_{y,l}\left(\widetilde{Y}_{i+l},Y_i^{i+l-1}\right)\right.$$
$$\left. - g^{\star}_y\left(\widetilde{Y}_{i+l},Y_i^{i+l-1}\right)\right| + \frac{\epsilon}{4}$$
$$\leq \frac{\epsilon}{2}. \qquad (49)$$

This concludes the proof of (37a). For (37b), note that

$$f^{\star}_{y,l} := \log\left(\frac{dP_{Y^l}}{d(P_{X^lY^{l-1}}\otimes\widetilde{P}_{Y_l})}\right)$$
$$= \log p_{Y_l|X^lY^{l-1}} - \log\widetilde{p}_{Y_l}, \qquad (50)$$

achieves the supremum. Following the same claims for $\widehat{\mathsf{D}}_{Y_l|Y^{l-1}X^l\|\widetilde{Y}_l}(D_n)$

$$\left|\widehat{\mathsf{D}}_{Y_l|Y^{l-1}X^l\|\widetilde{Y}_l}(D_n) - \mathsf{D}_{Y_l|Y^{l-1}X^l\|\widetilde{Y}_l}\right| \leq \frac{\epsilon}{2}, \qquad (51)$$

where

$$\widehat{\mathsf{D}}_{Y_l|Y^{l-1}X^l\|\widetilde{Y}_l}(D_n)$$

$$:= \sup_{g_{xy}\in\mathcal{G}_{\mathrm{tf}}^{XY}} \frac{1}{n}\sum_{i=0}^{n-1} g_{xy}\left(Y_i^{i+l}, X_i^{i+l}\right)$$

$$- \log\left(\frac{1}{n}\sum_{i=0}^{n-1} e^{g_{xy}\left(Y_i^{i+l-1}, X_i^{i+l}, \widetilde{Y}_{i+l}\right)}\right). \qquad (52)$$

With (51) and (49) we end the proof. ∎

C. Proof of lemma 1

Recall

$$\mathsf{D}_{Y_l|Y^{l-1}\|\widetilde{Y}_l} := \mathsf{D}_{\mathsf{KL}}\left(P_{Y_l|Y^{l-1}}\|\widetilde{P}_{Y_l}\Big|P_{Y^{l-1}}\right), \qquad (53\mathrm{a})$$

$$\mathsf{D}_{Y_l|Y^{l-1}X^l\|\widetilde{Y}_l} := \mathsf{D}_{\mathsf{KL}}\left(P_{Y_l|Y^{l-1}X^l}\|\widetilde{P}_{Y_l}\Big|P_{Y^{l-1}X^l}\right). \qquad (53\mathrm{b})$$

By expanding the first term we obtain,

$$\mathsf{D}_{Y_l|Y^{l-1}\|\widetilde{Y}_l}$$

$$= \mathbb{E}_{P_{Y^{l-1}}}\left[\mathsf{D}_{\mathsf{KL}}(P_{Y_l|Y^{l-1}}\|P_{\widetilde{Y}_l})\right]$$

$$= \int_{\mathcal{Y}^{l-1}}\left[\int_{\mathcal{Y}_l}\log\left(\frac{P(y_l|y^{l-1})}{\widetilde{P}(y^l)}\right)\right.$$

$$\left. P(y_l|y^{l-1})d(y_l)\right]P(y^{l-1})d(y^{l-1})$$

$$= \int_{\mathcal{Y}^l}\log\left(\frac{P(y_l|y^{l-1})}{\widetilde{P}(y_l)}\right)P(y^l)d(y^l)$$

$$= \int_{\mathcal{X}^l\mathcal{Y}^l}\log\left(\frac{P(y_l|y^{l-1})}{\widetilde{P}(y_l)}\right)P(x^ly^l)d(x^ly^l), \qquad (54)$$

and the second term,

$$\mathsf{D}_{Y_l|Y^{l-1}X^l\|\widetilde{Y}_l}$$

$$= \mathbb{E}_{P_{X^lY^{l-1}}}\left[\mathsf{D}_{\mathsf{KL}}(P_{Y_l|X^lY^{l-1}}\|P_{\widetilde{Y}_l})\right]$$

$$= \int_{\mathcal{X}^l\mathcal{Y}^{l-1}}\left[\int_{\mathcal{Y}_l}\log\left(\frac{P(y_l|x^ly^{l-1})}{\widetilde{P}(y_l)}\right)\right.$$

$$\left. P(y_l|x^ly^{l-1})d(y_l)\right]P(x^ly^{l-1})d(x^ly^{l-1})$$

$$= \int_{\mathcal{X}^l\mathcal{Y}^l}\log\left(\frac{P(y_l|x^ly^{l-1})}{\widetilde{P}(y_l)}\right)P(x^ly^l)d(x^ly^l), \qquad (55)$$

where $\widetilde{P}_Y$ is a reference density function and is absolutely continuous on $\mathcal{Y}$. Subtructing the two terms resulting,

$$\mathsf{D}_{Y_l|Y^{l-1}X^l\|\widetilde{Y}_l} - \mathsf{D}_{Y_l|Y^{l-1}\|\widetilde{Y}_l}$$

$$= \int_{\mathcal{X}^l\mathcal{Y}^l}\log\left(\frac{P(y_l|x^ly^{l-1})}{P(y_l|y^{l-1})}\right)P(x^ly^l)d(x^ly^l)$$

$$= h(Y_l|Y^{l-1}) - h(Y_l|X^lY^{l-1})$$

$$= \mathsf{TE}_{X\to Y}(l). \quad \square \qquad (56)$$

D. Proof of lemma 2

The optimal TE, $\mathsf{TE}_{X\to Y}^\star(l)$, by non-finite memory process $\mathbb{X}$, is given by

$$\mathsf{TE}_{X\to Y}^\star(l) := \lim_{n\to\infty}\sup_{P_{X_{-n}^l}}\mathsf{TE}_{X\to Y}(l). \qquad (57)$$

For any $n > 0$ we have,

$$\sup_{P_{X_{-n}^l}}\mathsf{TE}_{X\to Y}(l)$$

$$= \sup_{P_{X_{-n}^0}P_{X^l|X_{-n}^0}} \mathsf{I}\left(X^l; Y_l|Y^{l-1}\right)$$

$$= \sup_{P_{X_{-n}^0}P_{X^l|X_{-n}^0}} \int_{\mathcal{X}_{-n}^l\mathcal{Y}^l} P(x_{-n}^0)P(x^l,y^l|x_{-n}^0)$$

$$\underbrace{\mathsf{I}\left(X^l; Y_l|Y^{l-1}\right)}_{\text{independent of } x_{-n}^0} d(x^lx_{-n}^0y^l)$$

$$\overset{(a)}{=} \sup_{P_{X^l}} \int_{\mathcal{X}^l\mathcal{Y}^l} P(x^l,y^l)\mathsf{I}\left(X^l; Y_l|Y^{l-1}\right)d(x^ly^l)$$

$$= \sup_{P_{X^l}}\mathsf{TE}_{X\to Y}(l), \qquad (58)$$

where (a) follows from the fact that the conditional MI does not depend on x_{-n}^0, thus we can eliminate the integral of $\mathcal{X}_{-n}^0$ that does not affect the conditional MI, as for the supremum. Since (58) is true for any $n \in \mathbb{N}$, with (57) we get,

$$\mathsf{TE}_{X\to Y}^\star(l) = \sup_{P_{X^l}}\mathsf{TE}_{X\to Y}(l). \quad \square \qquad (59)$$

E. Implementation Parameters

For the channel capacity estimation model, we trained the optimization procedure with a limit of 200 epochs. We utilized a batch size of 1024, a learning rate of 8×10^{-3}, and the Adam optimizer [47]. The transformer architecture comprises one attention layer followed by a FF layer. The attention mechanism is implemented with a single head, having a dimension of 32 neurons. The dimension of the FF layer is 64, featuring ELU activation [48]. The input sequence length is set to 59, and we back-propagate through sequences of length 30, corresponding to the parameter l in TE. Each epoch generates 100K samples of channel input-output tuples, with random noise uniformly distributed over the bounds of a given batch. The noise distribution generator (NDG) also employs a transformer structure with one attention layer and one FF layer, maintaining the same dimensional specifications. The learning rate for the NDG is set to 8×10^{-4}. It is trained at a rate of once every four epochs.

For the Apnea dataset feature analysis, the learning rate was adjusted to 1×10^{-4}. Additionally, we configured the model to use 1 head with a dimension of 16 for the attention mechanism, and the FF layer dimension was set to 32, with ELU activation. All experiments were conducted on *Nvidia RTX 3090 GPUs*.

REFERENCES

[1] Thomas Schreiber. Measuring information transfer. *Physical review letters*, 85(2):461, 2000.

[2] JM Nichols. Examining structural dynamics using information flow. *Probabilistic Engineering Mechanics*, 21(4):420–433, 2006.

[3] Ping Duan, Fan Yang, Tongwen Chen, and Sirish L Shah. Direct causality detection via the transfer entropy approach. *IEEE transactions on control systems technology*, 21(6):2052–2066, 2013.

[4] T. R. J. Bossomaier, Lionel C. Barnett, Michael S. Harré, and Joseph T. Lizier. An introduction to transfer entropy. In *Cambridge International Law Journal*, 2016.

[5] Chulhee Yun, Srinadh Bhojanapalli, Ankit Singh Rawat, Sashank J Reddi, and Sanjiv Kumar. Are transformers universal approximators of sequence-to-sequence functions? *arXiv preprint arXiv:1912.10077*, 2019.

[6] Haixu Wu, Jiehui Xu, Jianmin Wang, and Mingsheng Long. Autoformer: Decomposition transformers with auto-correlation for long-term series forecasting. *Advances in Neural Information Processing Systems*, 34:22419–22430, 2021.

[7] Haoyi Zhou, Shanghang Zhang, Jieqi Peng, Shuai Zhang, Jianxin Li, Hui Xiong, and Wancai Zhang. Informer: Beyond efficient transformer for long sequence time-series forecasting. In *Proceedings of the AAAI conference on artificial intelligence*, volume 35, pages 11106–11115, 2021.

[8] Tian Zhou, Ziqing Ma, Qingsong Wen, Xue Wang, Liang Sun, and Rong Jin. Fedformer: Frequency enhanced decomposed transformer for long-term series forecasting. In *International Conference on Machine Learning*, pages 27268–27286. PMLR, 2022.

[9] Qingsong Wen, Tian Zhou, Chaoli Zhang, Weiqi Chen, Ziqing Ma, Junchi Yan, and Liang Sun. Transformers in time series: A survey, 2023.

[10] Boris Gourévitch and Jos J. Eggermont. Evaluating information transfer between auditory cortical neurons. *Journal of Neurophysiology*, 97(3):2533–2543, 2007. PMID: 17202243.

[11] Shinya Ito, Michael E Hansen, Randy Heiland, Andrew Lumsdaine, Alan M Litke, and John M Beggs. Extending transfer entropy improves identification of effective connectivity in a spiking cortical network model. *PloS one*, 6(11):e27431, 2011.

[12] M. D. Madulara, P. A. B. Francisco, S. Nawang, D. C. Arogancia, C. J. Cellucci, P. E. Rapp, and A. M. Albano. Eeg transfer entropy tracks changes in information transfer on the onset of vision. *International Journal of Modern Physics: Conference Series*, 17:9–18, 2012.

[13] Max Lungarella and Olaf Sporns. Mapping information flow in sensorimotor networks. *PLoS computational biology*, 2(10):e144, 2006.

[14] Greg Ver Steeg and Aram Galstyan. Information transfer in social media. In *Proceedings of the 21st international conference on World Wide Web*, pages 509–518, 2012.

[15] Sondo Kim, Seungmo Ku, Woojin Chang, and Jae Wook Song. Predicting the direction of us stock prices using effective transfer entropy and machine learning techniques. *IEEE Access*, 8:111660–111682, 2020.

[16] Paolo Bonetti, Alberto Maria Metelli, and Marcello Restelli. Causal feature selection via transfer entropy. *arXiv preprint arXiv:2310.11059*, 2023.

[17] Murray Rosenblatt. Remarks on some nonparametric estimates of a density function. *The annals of mathematical statistics*, pages 832–837, 1956.

[18] Lyudmyla F Kozachenko and Nikolai N Leonenko. Sample estimate of the entropy of a random vector. *Problemy Peredachi Informatsii*, 23(2):9–16, 1987.

[19] Alexander Kraskov, Harald Stögbauer, and Peter Grassberger. Estimating mutual information. *Physical review E*, 69(6):066138, 2004.

[20] Clive WJ Granger. Investigating causal relations by econometric models and cross-spectral methods. *Econometrica: journal of the Econometric Society*, pages 424–438, 1969.

[21] Lionel Barnett and Terry Bossomaier. Transfer entropy as a log-likelihood ratio. *Physical review letters*, 109(13):138105, 2012.

[22] Lionel Barnett, Adam B Barrett, and Anil K Seth. Granger causality and transfer entropy are equivalent for gaussian variables. *Physical review letters*, 103(23):238701, 2009.

[23] M. D. Donsker and S. R. S. Varadhan. Asymptotic evaluation of certain Markov process expectations for large time. iv. *Communications on Pure and Applied Mathematics*, 36(2):183–212, 1983.

[24] M. I. Belghazi et. al. Mutual information neural estimation. In *International Conference on Machine Learning*, pages 531–540. PMLR, 2018.

[25] Dor Tsur, Ziv Aharoni, Ziv Goldfeld, and Haim Permuter. Neural estimation and optimization of directed information over continuous spaces. *IEEE Transactions on Information Theory*, 2023.

[26] J. Zhang, O. Simeone, Z. Cvetkovic, E. Abela, and M. Richardson. Itene: Intrinsic transfer entropy neural estimator. *arXiv preprint arXiv:1912.07277*, 2019.

[27] Ashish Vaswani, Noam Shazeer, Niki Parmar, Jakob Uszkoreit, Llion Jones, Aidan N Gomez, Łukasz Kaiser, and Illia Polosukhin. Attention is all you need. *Advances in neural information processing systems*, 30, 2017.

[28] Jiaming Song and Stefano Ermon. Understanding the limitations of variational mutual information estimators. *arXiv preprint arXiv:1910.06222*, 2019.

[29] David McAllester and Karl Stratos. Formal limitations on the measurement of mutual information. In *International Conference on Artificial Intelligence and Statistics*, pages 875–884. PMLR, 2020.

[30] Kwanghee Choi and Siyeong Lee. Combating the instability of mutual information-based losses via regularization. In *Uncertainty in Artificial Intelligence*, pages 411–421. PMLR, 2022.

[31] Ying Liu and Selin Aviyente. The relationship between transfer entropy and directed information. In *2012 IEEE Statistical Signal Processing Workshop (SSP)*, pages 73–76. IEEE, 2012.

[32] J. Massey. Causality, feedback and directed information. In *Proc. Int. Symp. Inf. Theory Applic.(ISITA-90)*, pages 303–305. Citeseer, 1990.

[33] G. Kramer. *Directed information for channels with feedback*, volume 11. Citeseer, 1998.

[34] K. Hornik, M. Stinchcombe, and H. White. Multilayer feedforward networks are universal approximators. *Neural networks*, 2(5):359–366, 1989.

[35] S. Molavipour, H. Ghourchian, G. Bassi, and M. Skoglund. Neural estimator of information for time-series data with dependency. *Entropy*, 23(6):641, 2021.

[36] Ke Bai, Pengyu Cheng, Weituo Hao, Ricardo Henao, and Larry Carin. Estimating total correlation with mutual information estimators. In *International Conference on Artificial Intelligence and Statistics*, pages 2147–2164. PMLR, 2023.

[37] Roland L. D. General formulation of Shannon's main theorem in information theory. *American mathematical society translations*, 33:323–438, 1963.

[38] Sekhar Tatikonda and Sanjoy Mitter. The capacity of channels with feedback. *IEEE Transactions on Information Theory*, 55(1):323–349, 2008.

[39] A. El Gamal and Y. H. Kim. *Network information theory*. Cambridge university press, 2011.

[40] T. M. Cover and J. A. Thomas. *Elements of Information Theory*. Wiley, New-York, 2nd edition, 2006.

[41] S. Yang, A. Kavcic, and S. Tatikonda. On the feedback capacity of power-constrained gaussian noise channels with memory. *IEEE Transactions on Information Theory*, 53(3):929–954, 2007.

[42] O. Sabag, V. Kostina, and B. Hassibi. Feedback capacity of mimo gaussian channels. *arXiv preprint arXiv:2106.01994*, 2021.

[43] DR Rigney, AL Goldberger, WC Ocasio, Y Ichimaru, GB Moody, and RG Mark. Multi-channel physiological data: description and analysis. In AS Weigend and NA Gershenfeld, editors, *Time Series Prediction: Forecasting the Future and Understanding the Past*, pages 105–129. Addison-Wesley, Reading, MA, 1993.

[44] A Goldberger, L Amaral, L Glass, J Hausdorff, PC Ivanov, R Mark, and HE Stanley. Physiobank, physiotoolkit, and physionet: Components of a new research resource for complex physiologic signals. *Circulation [Online]*, 101(23):e215–e220, 2000.

[45] Dor Tsur, Bashar Huleihel, and Haim Permuter. Rate distortion via constrained estimated mutual information minimization. In *2023 IEEE International Symposium on Information Theory (ISIT)*, pages 695–700. IEEE, 2023.

[46] L. Breiman. The individual ergodic theorem of information theory. *The Annals of Mathematical Statistics*, 28(3):809–811, 1957.

[47] Diederik P Kingma and Jimmy Ba. Adam: A method for stochastic optimization. *arXiv preprint arXiv:1412.6980*, 2014.

[48] Djork-Arné Clevert, Thomas Unterthiner, and Sepp Hochreiter. Fast and accurate deep network learning by exponential linear units (elus). *arXiv preprint arXiv:1511.07289*, 2015.